Final report

for the

Marshallplan-Jubiläumsstiftung

submitted by

Valerie Plajer, B.Sc.

based on

Valerie Plajer's Master Thesis

"The role of long non-coding RNAs in

CD8 T cell-mediated immunity"

performed in the laboratory of

Prof. Richard A. Flavell

Department of Immunobiology

Yale School of Medicine

300 Cedar Street, New Haven

CT 06520, U.S.A.

The Master's thesis
"The role of long non-coding RNAs in CD8 T cell-mediated immunity"
was partially modified by me, Valerie Plajer to serve as
a final report of my work at the Yale School of Medicine
for the Austrian Marshall Plan Foundation.

I was supervised by Dr. Dietmar Herndler-Brandstetter,
a Postdoctoral Fellow and Associate Research Scientist in the lab.

Table of contents

1. ACKNOWLEDGEMENTS

I would like to officially thank the Austrian Marshall Plan Foundation for financially supporting my research stay in the United States of America and therefore allowing me to perform my master thesis under the supervision of Dr. Dietmar Herndler-Brandstetter at the renowned laboratory of Prof. Richard A. Flavell at the Department of Immunobiology at Yale School of Medicine.

2. ABSTRACT

Recently, long noncoding RNAs (lncRNAs) have become a topic of general interest in research fields such as epigenetics, developmental biology and cancer biology. Due to the decisive role of lncRNAs as posttranscriptional regulators and their cell- and tissue-specific expression patterns, we have decided to study their functional relevance in the context of cytotoxic T lymphocyte-mediated immunity during infection. As the immune response is based on a complex network of interaction, activation and migration of different cells types to eliminate pathogens and establish long-term immunity, we performed deep RNA-seq and identified several lncRNAs that were regulated in cytotoxic T lymphocytes during infection *in vivo*. To study their role *in vivo*, we generated six lncRNA knockout mice using CRISPR/Cas9-mediated genome engineering. Here, I present data analyzing the functional role of *lncRNA-111*, *lncRNA-117* and *lncRNA-124* in knockout mice in steady state and following bacterial infection.

3. INTRODUCTION

3.1 THE IMMUNE SYSTEM: A BRIEF SYNOPSIS

The immune system has the vital function to protect an organism from infectious agents and malignant cells. It consists of an innate and an adaptive component[1].

The innate immune response is the first line of defense. Within the first hours to days of an infection, different phagocytic cells, like neutrophils, monocytes, macrophages and dendritic cells, are able to recognize, take up and kill pathogens. This rapid responsiveness is facilitated by their expression of pathogen recognition receptors, which recognize common antigens displayed by pathogens. At the same time, the innate immune system primes cells of the adaptive immune system. Dendritic cells, for example migrate to secondary lymphoid organs, present processed epitopes from the pathogen bound to major histocompatibility complex (MHC) molecules to cells of the adaptive immune system, and additionally provide them with co-stimulatory signals for their activation[1].

The adaptive immune system consists of B and T cells. It is known to cause a specific immune response against bacteria, viruses and parasites by recognizing distinct epitopes of the pathogen via unique antigen receptors.
B cells, once they are activated, can differentiate into plasma cells. These plasma cells produce immunoglobulins, which can either neutralize a pathogen or tag the pathogen (or infected cell) for faster recognition and destruction by other immune cells[1].
Mature T cells can be subdivided into two classes by distinct surface proteins: CD4 and CD8 T cells. CD4 T helper cells can recognize antigens in the context of MHC class II molecules. Naïve T helper cells can differentiate into T_H1, T_H2, T_H17 and T_{FH} cells after stimulation by an antigen-presenting cell (APC). These effector CD4 T cell subsets differ from each other in terms of their cytokine production, but also in terms of their role in the immune response: They can play a crucial role in the recruitment of different innate

immune cell types to the site of infection as well as in the activation of B and CD8 T cells.
CD8 cytotoxic T cells, also called cytotoxic T lymphocytes (CTLs), recognize antigens in the context of MHC class I molecules, which are expressed on all nucleated cells. If a cell is infected with an intracellular pathogen, activated CTLs can recognize and kill the infected cell[1].

3.1.1 Development of T cell receptor (TCR) αβ T cells in the thymus

Lymphoid progenitors give rise to both B and T cells. Instead of developing in the bone marrow (as do B cells), some progenitors migrate to the thymus where they give rise to two distinct lineages of T cells: αβ- and γδ-T cells[1].

Considering my thesis subject, I will only elaborate on the development of αβ T cells: First, every αβ-T cell has to pass 4 double negative (DN) stages, which can be distinguished by the differential expression levels of CD44 and CD25[2]. During the last two DN stages, the T cells form complexes of the pre-T cell receptor (pre-TCR) and CD3ε/ζ. Those complexes can now form dimers with one another, which trigger proliferation and subsequently initiate the switch to the double-positive (DP) stage[3].

The DP population has the highest cell count in the thymus and expresses both CD4 and CD8 co-receptors on their cell surface. During this stage, the alpha chain locus rearranges, which leads to the formation of mature TCRs. After that, the DP cells have to interact with cortical thymic epithelial cells, which present MHC class I and II molecules in complex with self-peptides on their surface. If the interaction with these cells triggers an intermediate TCR signal, the double positive cells survive (positive selection). However, if the signal is either too weak or too strong, it will lead to apoptosis of the double positive cells (death by neglect and negative selection) and therefore eliminate futile and self-reactive T cells. Due to the intensive screening, only 2% of the immature thymocytes actually become mature single positive T

cells; These can leave the thymus and migrate to secondary lymphoid organs as either naïve CD4 or CD8 single positive T cells[1,3].

3.1.2 The CD8 T cell response to pathogens

Once an APC displays a pathogenic epitope on a MHC class I molecule and co-stimulatory signals to a naïve CD8 T cell with the appropriate high affinity TCR, the T cell response, which consists of three distinguishable phases, is initiated. First, the activated naïve T cells start to proliferate (phase 1: clonal expansion) and differentiate into short-lived effector precursors (SLECs) and memory precursor effector cells (MPECs). This is modulated by signals like antigen binding, different co-stimulators and pro-inflammatory signals like cytokines (type I interferons (IFNs), IFN-γ, interleukin (IL)-2 etc.). The strength and persistence of each signal can influence the composition of effector T cell subsets as well as the quality, quantity and lifespan of memory T cells.

Subsequently, following specific chemokine gradients, the activated effector T cells can leave the secondary lymphoid organ and migrate to the site of infection. Once they arrive there, the CD8 T cells can recognize infected cells by their display of pathogenic peptides in complex with MHC class I molecules. The additional interaction of ICAM-1 with LFA-1 initiates the formation of an immunological synapse between the cytotoxic T cell and the target cell without the need for co-stimulatory signals.[1,4,5,6]

Activated CD8 T cells contain cytotoxic granules, which have three classes of effector proteins: Perforin, which can form pores in the plasma membrane of the target cell, granzymes, which can activate caspases and induce apoptosis, and granulysin, which disrupts the membrane of infected cells and microbes, but is absent in mice. The cytotoxic granules are first generated during the initial interaction between the naïve T cell and the target antigen-MHC complex presented by an APC. Once the immunological synapse forms with an infected cell, the secretion of the granules is oriented in the same direction, which allows the T cell to specifically target and kill one cell and does not harm any of the uninfected neighboring cells. Granzyme B induces

DNA degradation and subsequent apoptosis in the infected cell. Phagocytes recognize a change in the cell membrane and take up the dying cells. Cytotoxic T cells also produce cytokines like IFN-γ, tumor necrosis factor (TNF)-α and lymphotoxin (LT)α to help clear an infection. IFN-γ can increase the amount of MHC class I molecules displayed on the cell surface as well as inhibit the viral replication cycle. TNF-α and LTα can activate macrophages or interact with TNFR-1, which subsequently leads to cell death. Also the expression of Fas ligand on cytotoxic T cells causes the activation of caspases in infected cells, if it binds to Fas receptor.[1,6]

After the infection is resolved and the vast number of effector CD8 T cells is not required anymore, most of them die due to apoptosis (Phase 2: contraction phase). Only 5-10% of the cells survive this phase and become memory CD8 T cells (Phase 3: memory formation). As of now, complete comprehension of the crucial difference between the cells that survive and those who die has not been reached, but there are multiple models which try to explain this process (not shown here)[4].
Memory CD8 T cells are currently being divided in three groups: The central memory T cells (T_{CM}) reside mostly in the secondary lymphoid organs and they are identified by their CD62L^{hi} CCR7^{hi} expression. The advantage of T_{CM} cells is their generation of large amounts of effector cells once they are reactivated. The effector memory T cells (T_{EM}) express CD62L^{low} CCR7^{low} and show higher similarity to effector T cells due to their enhanced cytotoxic function. Tissue resident memory T cells (T_{RM}) expressing CD103^{hi} CD69^{hi} CD27^{low} are known to reside directly in organs (such as the lung and the intestinal mucosa) and can have direct effector functions additionally to the T_{EM} cells[7,8,9].
Cytokines like IL-7 and IL-15 are important factors for the survival and self-renewal of memory CD8 T cells. They allow the immune system to maintain antigen-specific T cells for a long period of time after an infection, which can rapidly react if re-challenged with the same pathogen[10].

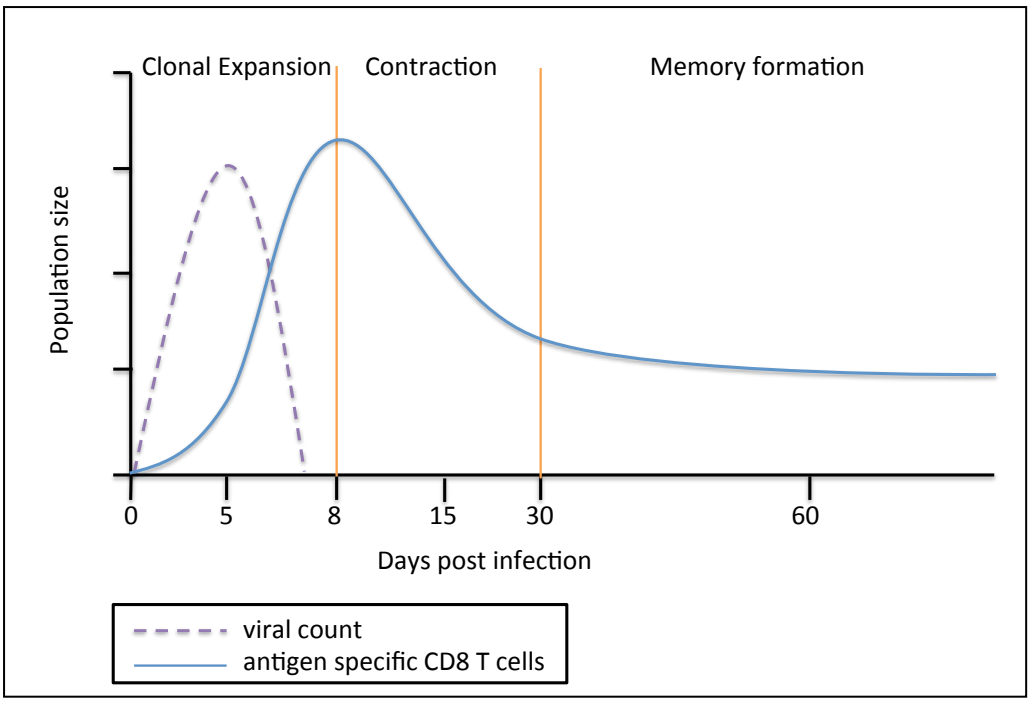

Figure 3.1 The CD8 T cell response to pathogens
The graph depicts the course of T cell expansion, contraction and memory formation during and after the infection with a virus. The T cell population expands until day 8, after which the infection should be cleared. Afterwards, the population of antigen specific T cells contracts until only 5-10% of it remains, which form the memory CD8 pool. Adapted from S. Kaech and W. Cui (2012)[4]

3.1.3 *Listeria monocytogenes* as a model pathogen for bacterial infections

Listeria monocytogenes is a gram-positive, facultative intracellular and opportunistic bacterium that is pathogenic for humans and animals[11–13].
It was first discovered in 1926 in Cambridge, where it caused the death of a rabbit colony by inducing monocytosis[13,14]. This lead to its first name: *Bacterium monocytogenes*. A few years later, it was found causing necrotizing hepatic infections in wild animals in South Africa, where it was named *Listeria hepatolytica* in honor of the British surgeon Joseph Lister. As they realized that both outbreaks were caused by the same pathogen, they combined the names to *Listeria monocytogenes*[14].

Listeria can also cause different diseases in humans depending on the affected person as well as its route of infection: It can infect immunocompromised and elderly people, where it can cause gastroenteritis,

meningitis, encephalitis or septicemia. In pregnant women it can also lead to mother-to-fetus infections[12,14]. The natural route of infection is through oral uptake of contaminated food[14]. In humans, the bacteria can cross the epithelial cell layer of the gastrointestinal tract by the binding of bacterial Internalin A to human E-Cadherin on epithelial cells and the subsequent entering of either the lymph or blood stream to finally reach the liver and spleen. Once in the liver or spleen, the bacteria are either internalized by macrophages or enter non-phagocytic cells of the tissue on their own. Due to the change of one amino acid in the murine E-Cadherin, Internalin A cannot bind to it, preventing the bacteria from crossing the gastrointestinal barrier. To overcome this problem when using a mouse model, the bacterium is either injected intravenous or intraperitoneal, which causes a systemic infection[14].

Listeria can escape vacuoles and phagosomes by producing the pore-forming toxin Listeriolysin O (LLO). Once in the cytosol, it expresses actin-assembly-inducing protein (ActA), which causes the nucleation of cellular actin. This allows the bacteria to move through the cytoplasm and even into neighboring cells[14]. While *Listeria* is present in the cytosol, its secreted proteins can be processed by the host proteasome. The complex of a *Listeria* epitope with a MHC class I or II molecule is then transported to the surface of the infected cell, where it can be recognized and bound by specific TCRs on T cells[15]. The CD8 T cells lyse the infected cells and secrete IFN-γ to activate macrophages, which leads to clearance of the infection, immunological T cell memory and thereby enhanced resistance upon re-challenge in the future[15,16]. LLO has an epitope that shows a specific MHC class II restriction for C57BL/6 mice and therefore causes a strong CD4 T cell response. Since there is no strong MHC class I restricted epitope for C57BL/6 mice known, recombinant *Listeria* strains have been generated which express foreign H2-K^b epitopes derived e.g. from Ovalbumin (OVA)[15]. This allows researchers to use *Listeria monocytogenes* as a model to study cytotoxic T cell immune responses.

3.2 LONG NONCODING RNAS

It is known that roughly 80% of our DNA is functional[17]. While the newest GENCODE statistic suggests that only approximately 20,000 genes in humans encode for proteins, pseudo genes and noncoding RNAs account for the vast majority of the genome[18].
Main players are the long noncoding RNAs (lncRNAs), which comprise approximately 16,000 genes in the human genome[18]. LncRNAs are by definition longer than 200 nucleotides and in general do not encode any proteins[19]. If compared to mRNAs, lncRNAs contain less but longer exons and are expressed at lower levels[20]. Nevertheless, lncRNAs are transcribed, capped and spliced like mRNAs[21].

The growing interest in lncRNAs is not only motivated by the fact that they are encoded by numerous genes and that their functionality has been disregarded up to a decade ago, but also by the discovery that many lncRNAs seem to have specific expression patterns: It has been shown that their expression levels are highly diverse depending on the cell type and stage of development[20]. In the future, this characteristic could therefore be used to define cell types more accurately than by using protein-coding genes[22].

An aspect that complicates lncRNA research is the low conservation of long noncoding RNAs across different species. While their promoters and expression patterns can be highly conserved, their sequence is in general rapidly evolving and can therefore be highly variable between different species[21]. This impedes the direct translation of their function from rodents to humans. The extent in which the variability in lncRNAs does have an influence on the interspecies differences has yet to be discovered.

LncRNAs are categorized depending on their localization in regard to coding genes: Some lncRNAs are located within introns of protein-coding genes and are therefore called long intronic noncoding RNAs (lincRNAs), while some lncRNAs overlap with protein-coding genes (overlapping lncRNAs). Others

are located between two genes (intergenic lncRNAs) and/or are complementary to nearby genes (antisense lncRNAs)[19].

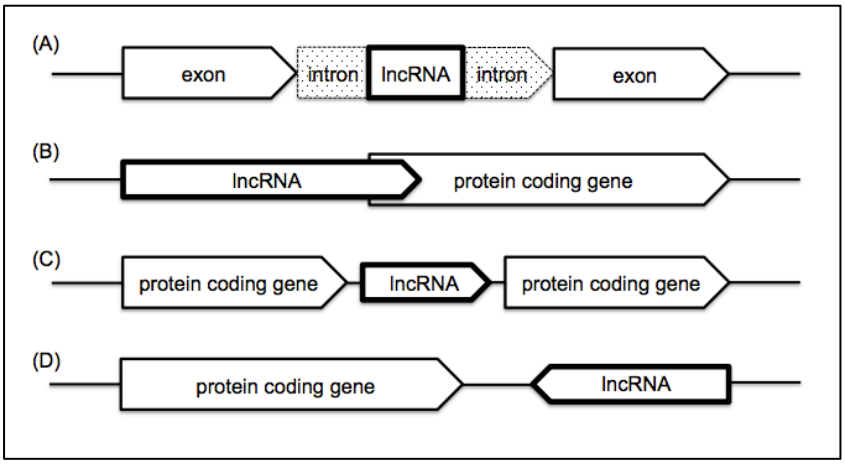

Figure 3.2 Illustration of the different types of lncRNAs
This figure shows the different localizations of lncRNAs: (A) long intronic noncoding RNA, (B) overlapping lncRNA, (C) intergenic lncRNA and (D) antisense lncRNA. Adapted from Fitzgerald and Caffrey (2015)[19].

3.2.1 The known functions of lncRNAs

Studies showed that lncRNAs play important roles as post-transcriptional regulators. They operate by binding to DNA sequences, RNAs or proteins[23]. On the one hand, this allows them to directly interact with their targets like *lnc-DC* does with STAT3, which prevents dephosphorylation of STAT3[24]. On the other hand, they can act as decoys like *PANDA* does for the transcription factor NF-YA, thus preventing apoptosis[25]. They can also interact with chromatin regulator complexes like *NeST* does with WDR5 (see 3.2.2)[26] or ribonucleoproteins (RNPs) like *lincRNA-p21* with hnRNP-K, which causes transcriptional gene repression[27].

The localization of the transcribed long non-coding RNA inside the cell can be used as an indicator for its function: nuclear lncRNAs can associate with chromatin modifying complexes, while cytoplasmic lncRNAs can post-transcriptionally regulate the transcript stability or the translation of the target itself[22].

Studies have shown that some lncRNAs can act in cis, like *lincR-Ccr2-5´AS'* (3.1.2.2), or in trans, like *NeST* (see 3.2.2), on neighboring genes[20].

Therefore, the vicinity to specific protein-coding genes is used to predict the function of yet undefined lncRNAs and to assign names[28]. To assess the chance of an existing correlation, the expression patterns of the lncRNA and the possible target gene can be compared via BioGPS data or independent qPCR analysis[29].

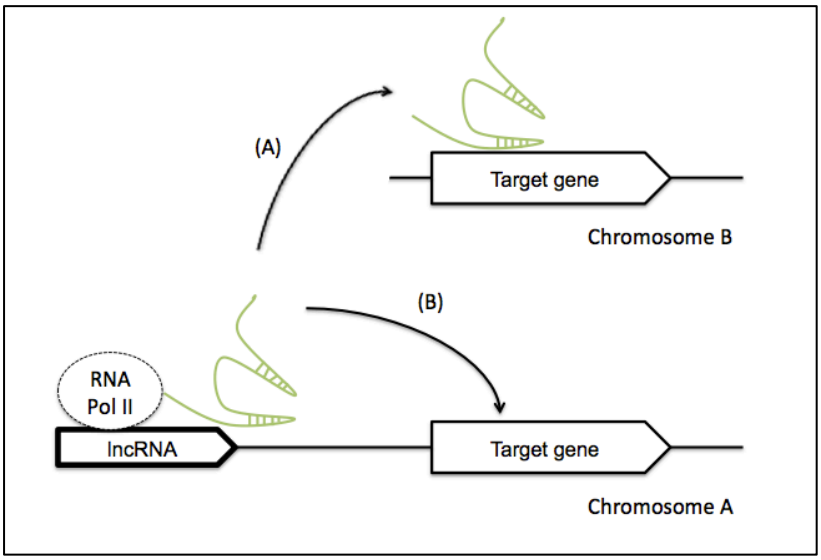

Figure 3.3 Illustration of the possible modes of interaction between a lncRNA and its target gene *Illustration of the trans (A) or cis (B) interaction of a lncRNA with its target gene. Adapted from Lam and Glass (2014)[65].*

3.2.2 The role of lncRNAs in the immune system

It was proposed that lncRNAs play a substantial role in the immune response by modulating the expression and/or function of crucial genes. Therefore, it could be possible that mutations in lncRNAs influence the development of autoimmune diseases, allergies and chronic diseases[20]. Another hypothesis suggests that the low interspecies conservation of lncRNAs is the main reason for the vast differences between e.g. the mouse and the human immune system[28].

There is a large number of lncRNAs that are lymphoid-specific and are differentially expressed between the different types of immune cells. The analysis of 42 different T cell subsets demonstrated that half of the expressed lncRNAs were cell type specific, whereas only 6-8% of mRNAs were[21].

An example for a lncRNA that plays a major role in the immune system is the enhancer-like *NeST* lncRNA. *NeST* regulates *Ifng* expression in T_H1 cells, in $CD8^+$ T cells and natural killer cells through binding to WDR5. WDR5 is a

component of the histone H3 lysine 4 methyltransferase complex, which causes a chromatin modification at the *Ifng* locus and thus induces its transcription[26].

Another example is *lincR-Ccr2-5´AS'*, which is activated by GATA3 in T_H2 cells. This lncRNA regulates the expression of genes preferentially expressed in T_H2 cells, such as specific chemokine receptors, which can alter the migration patterns of these T cells[30].

A disease related example is *lncRNA-CD244*, which has been discovered in tuberculosis-infected humans, where it regulates the expression of *Ifng* and *Tnfa* in CD8 T cells. The infection causes elevated levels of CD244, which then modify the chromatin state of the *lncRNA-CD244* gene to facilitate its transcription. The lncRNA can recruit the chromatin-modification enzyme EZH2 to the promoters of *Ifng* and *Tnfa. This* leads to their repression and, subsequently, an impaired CD8 T cell response[31].

3.2.3 Identification of lncRNAs that are regulated in CD8 T cells during infection

Deep RNA-seq analysis was performed on sorted OT-I cell subsets, which were purified from the spleen of mice during the course of a *Listeria monocytogenes* infection. The computational analysis was performed by the John Rinn laboratory at MIT and Harvard University. We identified lncRNAs that were differentially regulated between naïve, effector (SLECs and MPECs) and memory CD8 T cell subsets. To exclude possible unspecific lncRNAs and to minimize the number of candidates, only lncRNAs with an expression value of 20 FPKM or higher in at least one of the CD8 T cell subsets and with a differential expression greater than two between the subsets were chosen. The differential expression of seven lncRNAs was then verified by qPCR. None of the candidate lncRNAs overlapped with protein-coding genes. By using their expression patterns, the seven lncRNAs can be separated into 3 different groups (see Figure 3.4). Specific single-guide RNAs were designed to separately knock out the candidate lncRNAs in C57BL/6 mice using the CRISPR-Cas9 method (see 3.3)[32].

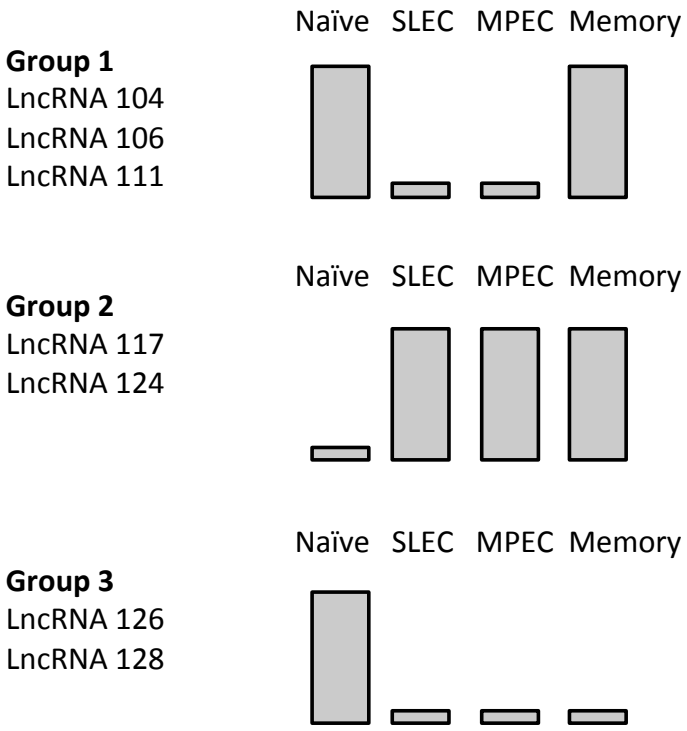

Figure 3.4 Expression patterns of candidate lncRNAs
The candidate lncRNAs can be subdivided into three different groups according to their expression patterns. This figure shows representative, simplified graphs for them: Group 1 shows elevated expression levels in naïve and memory CD8 T cells. Group 2 is highly expressed in activated CD8 T cells (short lived effector cells (SLEC), memory precursor effector cells (MPEC) and memory cells) and group 3 is highly expressed in naïve CD8 T cells only.
Adapted from Stecher (2015)[32].

Of the seven candidate genes, homozygous knockout mice were obtained for two lncRNAs (*lncRNA-117* and *lncRNA-124*). For four other candidate lncRNAs (*lncRNA-104*, *lncRNA-106*, *lncRNA-111* and *lncRNA-128*), heterozygous knockout mice are currently being bred to generate homozygous knockout mice.
This thesis will focus on three of the seven lncRNA candidates: *lncRNA-117*, *lncRNA-124* and *lncRNA-111*.

3.2.3.A LncRNA-117

The RNA-Seq analysis as well as the verification via qPCR showed that *lncRNA-117* is highly expressed in effector and memory CD8 T cells [32]. According to BioGPS, the organs with the highest expression levels are ovaries, followed by spleen, lymph nodes and lung[33]. Additionally, our own qPCR results showed high expression of *lncRNA-117* in the thymus[32]. Analysis of data acquired during another RNA-seq experiment in the Richard Flavell laboratory by Christian Harman, Jorge Henao-Mejia and Adam

Williams showed that this lncRNA is also highly expressed in T_H1 cells, natural killer T cells and B1a cells.

LncRNA-117 is located between two genes, here called gene *117-A* and gene *117-B*.
Gene *117-A* is highly expressed in the spleen, lymph nodes, bone marrow and lung. In the immune system, its highest expression is in follicular B cells and $FoxP3^+$ T regulatory cells[34].
Gene *117-B* is highly expressed in the testis and stimulated macrophages, and therefore has no correlation with the expression patterns of *lncRNA-117*[35].

3.2.3.B LncRNA-124

This lncRNA showed expression patterns comparable to *lncRNA-117* in the RNA-seq analysis: The expression increased after the CD8 T cells were activated following *Listeria monocytogenes* infection and stayed elevated until the memory phase. There are two different transcript variants, which show differences in the expression levels (transcript variant 1 is overall lower expressed than transcript variant 2), but their patterns are still coherent. Tissue expression analysis using qPCR revealed high expression in skin, bone marrow and thymus[32].

LncRNA-124 is located near the gene inhibitor of DNA binding 2 (*Id2*)[32]. ID2 is known for its importance in CD8 T cells: It is critical for the survival of effector CD8 T cells and the formation of $KLRG1^{hi}$ $IL7\text{-}R\alpha^{low}$ effector T cells. ID2 acts by modulating the expression of *Bcl2, Serpinb9* and *Bcl2l11*, all being apoptosis-associated genes[36,37].

About the other neighboring gene of *lncRNA-124*, the here called gene *124-A*, are no papers or expression patterns published yet.

3.2.3.C LncRNA-111

The RNA-seq analysis showed that the candidate *lncRNA-111* is highly expressed in quiescent cells. Therefore, its expression peaks in naïve and memory CD8 T cells, which was validated by qPCR analysis [32].
Additional RNA-seq analysis by Christian Harman showed that *lncRNA-111* is also highly expressed in T regulatory cells (T_{reg}) and neutrophils.

The tissue expression of *lncRNA-111* was analyzed by qPCR. Its highest expression was observed in lymph nodes and kidney, but also in the heart, thymus, lung and small intestine[32]. The BioGPS website has two files for the expression patterns of *lncRNA-111*: One probe set shows significantly higher expression of the lncRNA, with values higher than 10x the mean (mean value = 8.2), in the B cell marginal zone as well as the retinal pigment epithelium. In contrast, the other probe set shows enhanced expression, with expression levels higher than 3x the mean (mean value = 22.5), in CD4 and CD8 T cells, GL7 negative B cells, follicular B cells, mast cells and hematopoietic stem cells (HSC)[38].

One of its neighboring protein coding gene is the gene *111-A*. It is a cellular zinc transporter that is highly expressed in the stomach and gut, which is why it does not show any correlation with the candidate lncRNA regarding the expression patterns[39].
LncRNA-111 has a human orthologous, which is also upstream of the human *111-A* gene and shows high sequence conservation.

Another neighboring gene of *lncRNA-111* is the protein coding gene *Sox9* (SRY (sex determining region Y) box 9). Multiple papers have been published, that present an analysis of its function, which varies from being a transcriptional regulator for hair follicle stem cells to chondrocyte and heart valve development[40–42]. BioGPS data show three different probe sets, which all show the highest expression in lacrimal gland, salivary gland and prostate, varying from 3x to 30x the mean value.
Sox9 is also highly expressed in the retinal pigment epithelium (RPE), varying from 3x to 10x the mean value[43]. A study focusing on the expression of *Sox9*

in the eye showed that *Sox9* is highly expressed from early development on to the adult stage in the RPE[44]. In 2010 and 2014, Masuda and Esumi published two papers analyzing the functional role of *Sox9* in the RPE. According to their studies, it is an important regulator for the activation of the *BEST1* promoter, which if mutated can cause different diseases (VDM, AVDM, ADVIRC and ARB) all including visual impairment[45]. Additionally, they showed that *Sox9* is an important transcriptional regulator for several visual cycle genes in the RPE[46].

3.3 THE CRISPR-CAS9 TECHNOLOGY

Clustered regularly interspaced short palindromic repeat (CRISPR) technology is used to modify the genome with specific RNA-guided nucleases, like CRISPR-associated protein 9 (Cas9)[47].

Yoshizumi Ishino et al. first discovered CRISPR repeats in 1987: While analyzing the *iap* gene in *Escherichia coli*, they found 5 homologous sequences separated by spacers at the 3' end of the *iap* gene sequence. Since those repeats had never been characterized in prokaryotes before, Ishino et al. were not aware of the significance of their finding[48].
Those homologous repeats received their name CRISPR in 2002 by Ruud Jansen et al. The in silico analysis of different strains of bacteria and archaea showed a conservation of the repeats and the leader sequence next to CRISPR loci within one species, while there were interspecies variations. Even though they did not know about the functional relevance of CRISPR at that moment, they also identified 4 *Cas* genes and recognized their functional relationship with the CRISPR region[49].
Finally, in 2006, almost 20 years after the first description of the interspaced repeats, a paper was published by Kira S. Makarova et al., which revealed that the spacer sequences in CRISPRs are homologous to sequences in plasmid or virus genomes[50]. These results led to the understanding that CRISPR is the prokaryotic equivalent of the adaptive immune system.

If bacteriophages or plasmids invade a bacterium, various sequences of their DNA are incorporated between CRISPR repeats ("protospacer"). These DNA-CRISPR-elements are then transcribed into CRISPR RNAs (crRNAs), which form complexes with transactivating CRISPR RNAs (tracrRNA) and the Cas9 nuclease. The mature crRNA sequence recognizes invading, matching DNA next to protospacer adjacent motifs (PAMs) and the RNA guided nuclease Cas9 can initiate the cleaving process[47]. To mediate double strand breaks (DSB), both domains of the Cas9 enzyme have to be functional: The HNH domain cleaves the DNA strand to which the complimentary crRNA sequence binds via Watson-Crick pairing, while the RuvC-like domain cuts on the opposite strand[51].

Overall, there are three different CRISPR-Cas system types identified at the moment. The *Streptococcus pyogenes* type II system is most commonly used to modify the genome of model organisms. It encodes a tracrRNA: crRNA duplex, which allows a single protein to recognize and cleave the DNA[52].
This finding enabled the engineering of single guide RNAs (sgRNA): To modify a genome, only the last twenty nucleotides at the 5' end of a sgRNA have to be adjusted to target a specific sequence. In addition those nucleotides have to be adjacent to a PAM sequence (in *Streptococcus pyogenes*: 5'-N_{20}-NGG), which is essential for DNA binding[47]. These being the only required modifications makes CRISPR-Cas9 a more efficient genome-editing tool than the zinc finger nuclease (ZFN) or Transcriptional Activator-like Effector nuclease (TALENs) approach.

Genome editing takes advantage of intracellular mechanisms to modify the genome of a model organism for biological research purpose. First, enzymes like nucleases and nickases induce double strand breaks or single strand nicks (SSN). This damage is then repaired by endogenous DNA repair mechanisms, which either perform non-homologous end joining (NHEJ), leading to an insertion or deletion, or homology-directed repair (HDR), where the original sequence can be substituted by a partially homologous DNA template. HDR is the cornerstone of gene therapy, where a beneficial gene sequence replaces a harmful one[53].

The method can be used to study gene functions in single cell organisms, including bacteria and eukaryotes, as well as in cell cultures and whole organisms[47].
Since our goal is to study the importance of specific lncRNAs in CD8 T cells during an infection, we used CRISPR-Cas9 to generate lncRNA knockout mice.

3.4 AIMS

This work focuses on the *in vivo* analysis of three long non-coding RNAs that have previously been identified by deep RNA sequencing to be regulated in CD8 T cells during bacterial infection in mice. In previous experiments, it was shown that two candidate lncRNAs, *lncRNA-117* and *lncRNA-124*, were upregulated in activated CD8 T cells. In this study, we analyzed the phenotype of *lncRNA-117*$^{-/-}$ *and lncRNA-124*$^{-/-}$ mice during steady state and following bacterial infection.

For the third candidate lncRNA, *lncRNA-111*, we identified a possible inflammatory eye phenotype in *lncRNA-111*$^{+/-}$ mice and performed non-invasive experiments to characterize this phenotype.

4. MATERIALS AND METHODS

4.1 MATERIALS

4.1.1 Reagents and Buffers

4.1.1.1 DNA extraction

Name	Description
Quicktail lysis buffer	50 mM Tris pH 8.0 50 mM KCl 2.5 mM EDTA 0.45% NP40 0.45% Tween 20
Proteinase K	Sigma-Aldrich

4.1.1.2 PCR reagents

Name	Description
10x Tsg reaction buffer	Lamda Biotech
$MgCl_2$ buffer	25 mM, Lamda Biotech
dNTP	10 mM Lamda Biotech
Tsg DNA Polymerase	5 U/µL, Lambda Biotech

4.1.1.3 Agarose gel and Analysis

Name	Description
Agarose GPG/LE	American Bioanalytical, MA
10x TBE buffer [stock]	1 M Tris base 1 M Boric acid 0.02 M EDTA ddH_2O
Ethidium Bromide	Sigma-Aldrich
100bp DNA ladder	500 ng DNA/6µL/loading, Lamda Biotech
Orange G solution	see Methods 4.2.1.1

4.1.1.4 Surveyor Assay Kit

Kit Components
0.15M $MgCl_2$ Solution
Surveyor enhancer S
Surveyor nuclease
Stop solution

The Surveyor Mutation Detection Kit was bought from Integrated DNA Technologies (IDT).

4.1.1.5 Cell isolation

Name	Description
Collagenase D	*Clostridium histolyticum*, stock concentration 20 mg/mL Roche Diagnostic GmbH
1x DPBS	Dulbecco's Phosphate Buffered Saline (-) Calcium chloride (-) Magnesium chloride gibco by life technologies
1x RPMI Medium 1640	(+) L Glutamine gibco by life technologies
FBS	Fetal Bovine Serum F4135 Sigma-Aldrich
Heparin	250 U/mL
ACK lysis buffer	Ammonium-Chloride- Potassium Thermo Fisher Scientific

4.1.1.5.A SI-IELs isolation

Name	Description
HEPES-bicarbonate buffer (10x)	23.8 g HEPES (100mM final) 21 g sodium bicarbonate (250 m final) H_2O to 1 L adjust pH to 7.2 with HCl

DTE solution (≈60 mL/SI)	50 mL 10x HBSS (Ca_2^+ and Mg_2^+ free) 50 mL 10x HEPES-bicarbonate buffer 50 mL FBS (heat inactivated) 350 mL H_2O Add 15.4 mg DTE /100 mL
Percoll	GE Healthcare Life Sciences diluted with ddH_2O to the preferred concentration

4.1.1.6 Spleen stimulation

Name	Description
PMA	Sigma-Aldrich
Ionomycin	Sigma-Aldrich

4.1.1.7 BD Cytofix/Cytoperm™ Fixation/Permeabilization Kit

Name	Description
BD Cytofix/Cytoperm™	1x Fixation and Permeabilization Solution BD Biosciences
BD Perm Wash™	Buffer stock: 10x solution BD Biosciences

4.1.1.8 Listeria monocytogenes overnight culture

Name	Description
LB media	Sigma Aldrich
Erythromycin	2.5 µL/5 mL LB media (stock concentration 10 mg/mL)

4.1.1.9 Antibiotic treatment

Name	Description
Sterile Ophthalmic	Neomycin and Polymyxin B

Ointment	Sulfates, and Bacitracin Zinc Ophthalmic Ointment, USP Akorn
Enrofloxacin water	1.9 mL Baytril®/ 250 mL H_2O

4.1.1.10 RNA Purification

Name	Description
Cryotube™ vials	1,8 ml Thermo scientific
TRIzol® Reagent	ambion RNA by life technologies

The RNeasy® Mini Kit from Qiagen was used to isolate RNA from tissue.

Kit Components
Buffer RPE
Buffer RLT
Buffer RW1
RNase-free water
Collection Tubes (2 mL)
Collection Tubes (1.5 mL)
RNase Mini Spin Column

4.1.1.11 Cytoplasmic & Nuclear RNA Purification

Kit Components
Lysis Buffer J
Buffer SK
Wash Solution A
Elution Buffer E
Spin Columns
Collection Tubes
Elution Tubes (1.7 mL)

The Cytoplasmic & Nuclear RNA Purification Kit from the Noreen Biotek Corporation was used for this purification and the ingredients mentioned below had to be provided by the user.

Name	Description
2-Mercaptoethanol	Gibco™ Thermo Fisher Scientific
Ethanol	96-100%

4.1.1.12 cDNA synthesis

Name	Description
Oligo (dT) 12-18	500 µL/mL
DNTP mix	10 mM each
5x First-strand buffer	250 mM Tris-HCl, pH 8,3 375 mM KCl 15 mM $MgCl_2$
DTT	0.1 M
SuperScript™ II RT	1 µL = 200 units purified from *E.coli* containing modified pol gene from Moloney Murine Leukemia Virus

The listed reagents were provided either by the Flavell Lab itself or used from the SuperScript™ II Reverse Transcriptase kit (Invitrogen by life technologies).

4.1.1.13 RT PCR reagents

Name	Description
KAPA SYBR® FAST qPCR Master Mix	(2x) Universal Provided by KAPA Bio systems
FW & RV Primers	10 µM (see 4.1.3.2)
Template DNA	see 4.1.1.12
ddH_2O	

For the RT qPCR, the KAPA SYBR® FAST qPCR Kit from KAPA Biosystems was used.

4.1.2 Mouse Strains

The following mouse strains were maintained at the Yale School of Medicine Animal Resource Center (YARC). All experiments were conducted in accordance with the Yale Animal Care and Use Committee guidelines.
C57BL/6N wild type (WT) mice were obtained from Charles River, MA. Those mice were used for the generation and breeding of the lncRNA knockout mice.

Strain name	Abbreviation	Origin
B6.129X1-Gt(ROSA)26Sortm1(EYFP)Cos/J	YFP	The Jackson Laboratory #006148
B6.Cg-Gt(ROSA)26Sortm14(CAG-tdTomato)Hze/J	TOMATO	The Jackson Laboratory #007914
KLRG1 IRES-eGFP-Cre, C57BL/6 background	KLRG1CRE	Flavell Lab
B6.129S6-Rag2tm1Fwa Tg(TcraTcrb)1100Mjb, C57BL/6 background	RAG2/OT-I	Taconic

4.1.3 Primer and Oligonucleotides

All primers were synthesized by and ordered from Sigma-Aldrich (MO, USA).
Both, the forward and the reverse oligo sequences, are written in 5' - 3' sense.
Various knockout primers were designed to test for the absence of the candidate lncRNAs as well as wild-type primers to test for the cutting efficiency of the various guide RNAs. Those primers are not depicted here.

4.1.3.1 Other primers

The following primers were used to genotype the offspring of lncRNA knockout mice crossed to already existing reporter mouse strains.

4.1.3.3.A Primers used to genotype KLRG1^{Cre} reporter mice

Primer	Sequence Forward	Sequence Reverse	Product size
KLRG1 WT	ATTCACAGAAATGGCCTCCA	TTTGCCCAGATTTAGGCTTT	286bp
KLRG1 Cre^{+}	CTGTGTCTGGTGTGGCTGAT	TTTGCCCAGATTTAGGCTTT	507bp
RAG2 WT	GGGAGGACACTCACTTGCCAGTA	AGTCAGGAGTCTCCATCTCACTGA	263bp

RAG2 KO	CGGCCGGAGAACCTGCGTGCAA	AGTCAGGAGTCTCCATCTCACTGA	380bp
OT-I	CAGCAGCAGGTGAGACAAAGT	GGCTTTATAATTAGCTTGGTCC	300bp
YFP neg.	GGAGCGGGAGAAATGGATATG	AAAGTCGCTCTGAGTTGTTAT	600bp
YFP pos.	AAGACCGCGAAGAGTTTGTC	AAAGTCGCTCTGAGTTGTTAT	320bp
Tomato neg.	AAGGGAGCTGCAGTGGAGTA	CCGAAAATCTGTGGGAAGTC	300bp
Tomato pos.	CTGTTCCTGTACGGCATGG	GGCATTAAAGCAGCGTATCC	196bp

4.1.4 Antibodies

The following antibodies were used to stain cells for flow cytometry.

4.1.4.1 Antibodies used for flow cytometry

Antibody	Clone / Company	Label
B220	RA3-6B2 / BioLegend	PerCP APC-Cy7
CD3	145-2C11 / BioLegend	APC
CD4	OKT4 / BioLegend RM4-5 / BioLegend GK1.5 / BioLegend	PE-Cy7 PerCP Pacific Blue
CD5	53-7.3 / BioLegend	APC
CD8α	53-6.7 / BioLegend	FITC PE PE-Cy7 Pacific Blue APC APC-Cy7 PerCP
CD8β	YTS156.7.7 / BioLegend	PE
CD11b	M1/70 / BioLegend	Pacific Blue
CD11c	N418 / BioLegend	PE-Cy7
CD19	6D5 / BioLegend	FITC
CD25	7D1 / BD Pharmingen 3C7 / BioLegend	FITC PE-Cy7 APC

CD27	LG7F9 / eBioscience	FITC PE
CD43	1B11 / BioLegend	PE-Cy7
CD44	IM7 / BioLegend	FITC PE-Cy7 APC APC-Cy7
CD45.1	*A20 / BioLegend*	*Pacific Blue* *APC-Cy7*
Antibody	**Clone**	**Label**
CD45.2	*104 / BioLegend*	*FITC* *PE* *APC*
CD127 (IL-7Rα)	A7R34 / BioLegend	Biotin
CD62L	MEL-14 / BioLegend	PerCP
CD69	H1.2F3 / BioLegend	FITC PE
CD107a	1D4B / BioLegend	AF488 Pacific Blue
CD103	2E7 / BioLegend	PerCP
CD183	CXCR3-173 / BioLegend	PE-Cy7
FoxP3	FJK-16S / eBioscience	PE
GZMB	GB11 / BioLegend	APC
IFNγ	XMG1.2 / BioLegend	FITC PE Brilliant Violet 421
IgD	11-26c.20 / BioLegend	Pacific Blue
IgM	R6-60.2 / Pharmingen	PE
IL-2	JES6-5H4 / BioLegend	FITC PE APC
KLRG1	2F1/KLRG1 / BioLegend	APC PE-Cy7
Ki67	B56 / BD Pharmingen	APC
NK1.1	PK136 / BioLegend	PE

		APC
TCR β	H57-597 / BioLegend	PE-Cy7 APC-Cy7
TCR γδ	GL3 / BioLegend	PE-Cy7

4.2 METHODS

4.2.1 Genotyping

4.2.1.1 Orange G solution

For 100 mL Orange G, 20 g Ficoll PM400 powder (GE Healthcare) and 1 mL of 1 M Tris (pH 7) were added to 50 ml ddH_2O and it was kept in a 37°C water bath O/N. On the next day, 1.7 g Orange G powder (Sigma-Aldrich) was added. Once it was resuspended, it was filled up with ddH_2O till a total volume of 100 mL.

4.2.1.2 Sample preparation, PCR settings and analysis

First, either toe or ear samples from mice were lysed by using 200 µL of Quicktail lysis buffer supplemented with 400 µg/mL Proteinase K. The samples were kept at 56°C in a water bath overnight. The following day, the enzyme was heat-inactivated by placing the samples in a 95°C heat block for 5 minutes.
To analyze the samples, the following master mix was added to 1 µL of template DNA in PCR tubes:

Compound	**Amount**
ddH_2O	18.05 µL
10x Tsg reaction buffer	2.5 µL
25mM $MgCl_2$	1.5 µL
10mM dNTPs	0.5 µL
Forward & Reverse primer	1.25 µL
Tsg polymerase	0.2 µL
Total	***24 µL***

The following PCR protocol was used:

Initial denaturation	3"	95°C
35 cycles	30'	95°C
	1"	60°C
	1"	72°C
Final elongation	10"	72°C

The following modified PCR protocol was used for RAG2 specific primers:

Initial denaturation	3"	95°C
25 cycles	30'	95°C
	30'	55°C
	30'	72°C
Final elongation	10"	72°C

Subsequently, 6 µL of Orange G solution was added to each sample and the samples were loaded onto a 2% agarose gel. A 100 bp DNA ladder was used as a reference (180 V, 130 mAmp, 30-40 minutes).

4.2.2 Surveyor Assay

Surveyor Assays were performed to test the cutting efficiency of single guide RNAs. The Surveyor nuclease is highly specific for mismatches; if only one of two guide RNAs cuts at their target site, the sequence can't be deleted and the DNA strands religate. This leads to point mutations, which can be detected if CRISPR-Cas9 treated DNA strands form heterodimers with wild type strands. In that case, the nuclease cuts both strands at the 3' side of the base pair mismatches, which subsequently can be detected as two bands on the agarose gel[54].

Initially, a PCR reaction was performed using primers that specifically amplify either the 5' or 3' end of the target sequence, on which one of the single guide RNAs should have bound and cut. Therefore, twice the amount of master mix (*see 4.2.1.2*) was added to 2 µL of template DNA (total: 50 µL). In addition to the mutant samples, wild-type samples were amplified in the extent that 5 µL of it could be added to each sample as well as 25 µL could be tested on a gel after the first PCR.

The first PCR reaction proceeds as follows

	Time	Temperature
Initial Denaturation	3"	95°C
25 cycles	30'	95°C
	30'	60°C
	30'	72°C
Final Elongation	10"	72°C

Afterwards, 25 µL of each product were mixed with 6 µL of Orange G solution for the following analysis on a 2% agarose gel to confirm the amplification of the target sequence (180 V, 130 mAmp, 30-40 minutes).

In the next step, 5 µL of each mutant sample that showed a single band of the correct size were transferred into a new PCR tube and 5 µL of wild-type product were added. Additionally, a control with 10 µL of wild-type product was prepared. The following program was used in the next step to obtain heterodimers of wild type and mutant DNA.

Time	Temperature
10"	95°C
1"	85°C
1"	75°C
1"	65°C
1"	55°C
1"	45°C
1"	35°C
1"	25°C
Hold	4°C

Immediately afterwards, the following master mix was added to each 10 µL DNA sample.

Compound	Amount
$MgCl_2$	1 µL
Surveyor Enhancer S	1 µL
Surveyor Nuclease S	1 µL

The PCR tubes were incubated at 42°C for 1 hour and subsequently, 1 µL of Stop Solution was added to inhibit nuclease activity. The products were tested on a 3-3.5% agarose gel (180 V, 130 mAmp), of which pictures were made every 20 minutes for one hour to see a clear separation of bands.

4.2.3 Flow cytometry

Flow cytometry was used to analyze distinct cell populations as well as their prevalence in different organs.

4.2.3.1 Cell isolation

Mice were euthanized using a CO_2 chamber and subsequently sprayed with 70% ethanol. The organs were harvested and kept in 1x DPBS on ice until the following cell isolation.

4.2.3.1.A Cell isolation from the Spleen

The spleen was transferred onto a petri dish. To isolate the cells from the maintaining tissue structure, a 70 µm mesh was put on top of the spleen before it was mashed with the flat end of a 10 mL plastic syringe. The extracted cells were rinsed in 4 mL 1x DPBS and transferred to a FACS tube.

4.2.3.1.B Cell isolation from the Bone marrow

Tibia and femur were cleaned from muscle tissue and cut open on both ends. To extract the bone marrow, it was flushed out with 1x DPBS using a 10 mL plastic syringe with a 27 G needle. The bone marrow was flushed into FACS tubes until the bones did not show any reddish bone marrow residues anymore.

4.2.3.1.C Cell isolation from the Lymph nodes

The axial and brachial lymph nodes were transferred onto a petri dish. To isolate the cells from the maintaining tissue structure, a 70 µm mesh was put on top of them before they were mashed with the soft end of a 10 mL plastic syringe. The extracted cells were rinsed in 3 mL 1x DPBS and transferred to a FACS tube.

4.2.3.1.D Cell isolation from the Lung

To isolate cells from the lung, the organ was cut into small pieces and kept in a 50 mL Falcon tube containing 5 mL of 1x RPMI medium + 10% FBS and Collagenase D (final concentration 1 mg/mL) in a shaker (37°C for 1 hour at 250 rpm).
Afterwards, the sample was vortexed and transferred through a mesh into a FACS tube.

4.2.3.1.E Cell isolation from the Liver

To isolate cells from the liver, the organ was meshed using the flat end of a 10 mL plastic syringe and kept in a 50 mL Falcon tube with 10 mL of 1x RPMI medium + 10% FBS in a shaker (37°C for 1 hour at 250 rpm). Afterwards, the sample was transferred through a mesh into a new Falcon tube.

4.2.3.1.F Isolation of intraepithelial lymphocytes (IELs) from the small intestine (SI)

The small intestine was cut into two halves and the feces were flushed out with 1x DPBS. Afterwards, it was cut open lengthwise to expose the intestinal mucosal layer and then cut laterally into 0.5 cm long pieces, which were transferred into 50 mL Falcon tubes containing 25 mL DTE solution. These tubes were kept at 37°C for 20 minutes while they were shaken at 220 rpm. Afterwards, the plastic tubes were vortexed for 15 seconds before transferring the solution through a 70 µm cell strainer into a new Falcon tube. The tubes were centrifuged at 1500 rpm for 5 minutes at 4°C, the supernatant was discarded and the pellet was resuspended in 5 mL 90% Percoll solution.
For each small intestine sample new 15 mL tubes were prepared by coating them with FBS, which has to be completely aspirated before the next step.
The 5 mL Percoll solution containing the IELs were transferred to the coated tubes and subsequently carefully underlaid with 7 mL 40% Percoll. The gradient was centrifuge for 20 minutes at 2400 rpm at 22°C without a brake. Afterwards, the remaining epithelial cells were aspirated from the top of the gradient and then the IELs were extracted, which are located at the interface of the 40% and 90% Percoll solutions. They were transferred into FACs tubes and washed once with 1 mL RPMI media + 10% FBS, followed by a centrifugation step and dilution of the pellet in 100 µL RPMI media + 10% FBS.

This protocol is based on the paper "Isolation of Mouse Lymphocytes from Small Intestine Tissues" by Brian S. Sheridan and Leo Lefrançois[55].

4.2.3.1.G Cell isolation from the peripheral blood

The peripheral blood sample was kept in a FACs tube with 50 µL of heparin. For the isolation of lymphocytes, the red blood cell lysis protocol (*see 4.2.3.3*) was performed two times with no processing steps in advance.

4.2.3.2 Blood count

To obtain a complete blood count, 20 µL of each peripheral blood sample are analyzed with Heska HemaTrue hematology Analyzer before the red blood cell lysis is performed. This analysis covers multiple cell subgroups and factors (for more information see https://www.heska.com).

4.2.3.3 Red Blood Cell lysis

To purify the samples of spleen, bone marrow, lung, liver and the peripheral blood the red blood cells (RBCs) were lysed.
Following the cell isolation steps (*see 4.2.3.1*), all tubes except for the peripheral blood were centrifuged (4°C for 5 minutes at 1500 rpm) and supernatants were discarded.
After that, 1 mL ACK lysis buffer was added to each pellet, they were resuspended and after 2 minutes 1 mL of cold 1x DPBS was added. After vortexing each sample, the tubes were centrifuged again (4°C for 5 minutes at 1500 rpm) and the supernatants were discarded.

4.2.3.4 Cell count

Cell count was performed for the samples of each organ except for the peripheral blood. Accuri® C6 Flow Cytometer was used with the CFlow Sampler software.

4.2.3.4.A Cell count for spleen, bone marrow, lung, liver and small intestine

After the lysis of RBCs, the pellet was resuspended in 1 mL of RPMI medium + 10% FBS and a specific amount was used for cell counting depending on the expected cell density of the samples (dilution with RPMI medium + 10% FBS). The remaining sample was spun down (4°C for 5 minutes at 1500 rpm) and the pellet was resuspended; 50 µL cold 1x DPBS was added before the following cell staining.

4.2.3.4.B Cell count for lymph nodes

From the 3ml of suspended lymph node, 50 µL was used for cell counting (diluted 1:1 in RPMI medium + 10% FBS). The remaining sample was spun down (4°C for 5 minutes at 1500 rpm) and the pellet was resuspended in 50 µL cold 1x DPBS before the following cell staining.

4.2.3.5 Stimulation of splenocytes

To analyze the ability of isolated T cells to produce interferon gamma and Granzyme B, splenocytes (obtained following the protocol of 4.2.3.1.A) were stimulated with PMA (30-50 ng/µL) and Ionomycin (500 ng/mL). For each sample, also an unstimulated control was prepared as comparison.
After 4.5 hours of stimulation in a 37°C incubator (5% CO_2), the samples were washed with 1x DPBS, spun down (4°C for 5 minutes at 1500 rpm) and resuspended in 50 µL cold 1x DPBS.

4.2.3.6 Cell staining

To stain the distinct cell populations, a mixture of specific antibodies (see 4.1.4.1) was added to each sample and incubated for 30 minutes. Afterwards, 1 mL of cold DPBS was added to the samples and they were spun down (4°C for 5 minutes at 1500 rpm).
Depending on the cell count, the samples were resuspended in amounts varying between 50-250 µL DPBS and kept on ice until flow cytometry was performed.

Intracellular staining

After the incubation with surface antibodies and the washing step with DPBS, 250 µL of 1x BD Cytofix/Cytoperm™ was added to each sample. After 30 minutes, 1 mL of 1x BD Perm Wash™ was added to each sample, they were spun down (4°C for 5 minutes at 1500 rpm) and the intracellular antibodies, diluted in 1x BD Perm Wash™, were added to each sample. After 20 minutes, another washing step and the subsequent centrifugation were performed and the pellet was diluted in RPMI medium supplemented with 10% FBS.

4.2.3.7 Flow cytometry and analysis

The flow cytometry analysis was performed on a BD LSR-II flow cytometer using the BD FACSDIVA™ software.
Subsequently, for precise analysis of the different cell populations, FlowJo software (version 10.1) was used. For further data analysis, Microsoft Excel® for Mac 2011 (version 14.4.5) and GraphPad Prism 6 for Mac OS X (version 6.0d) were used.

4.2.4 *Listeria monocytogenes* infection

To study the influence of lncRNAs during infection, the ovalbumin-expressing *Listeria monocytogenes* (LM-OVA*)* was used to promote the activation of the adaptive immune system and the generation of effector and memory CD8 T cells.
Since LM-OVA is a pathogen, all the following steps were performed in biosafety level 2 cabinets.
One day before the start of the experiment, an overnight (O/N) culture of LM-OVA was set up. A 50 µL LM-OVA bacterial suspension was transferred to a 50 mL plastic tube containing 5 mL LB media supplemented with 2.5 µL Erythromycin. The 50 mL plastic tube was placed into a sealed secondary container containing paper towels, which was placed in a shaking incubator at 37°C. On the next day, 10 µL and 50 µL of the O/N culture were added to 50 mL tubes containing each 5 mL LB media. These subcultures were placed in the shaking incubator for another 4.5 to 5 hours. Afterwards, the concentration of *L. monocytogenes* was measured using a spectrophotometer. With the measured OD_{600} value, the LM-OVA suspension was diluted with 1x DPBS. Each mouse received a retro-orbital injection of 100 µL with a final concentration of $1x10^6$ bacteria/mL.

4.2.5 RNA extraction

4.2.5.1 RNA extraction

For this experiment, the harvested organs were transferred into Cryotube™ vials containing 750 µL TRIzol® reagent and were snap frozen in liquid nitrogen. The following steps were done according to the instructions of the main protocol from the RNeasy® Mini Kit from Qiagen (see 4.1.1.10).

4.2.5.2 RNA extraction from the cytoplasm and nucleus

This experiment was done following the protocol from the Norgen Biotek Corp. kit (see 4.1.1.11) for cytoplasmic and nuclear RNA purification from animal tissues.

4.2.6 cDNA synthesis and RT-qPCR

First, the RNA levels and purity of the samples obtained during *4.2.5* were measured using the NanoDrop ND-1000 Spectrometer (Software: NanoDrop 3.1.2).
Using the SuperScript II Reverse Transcriptase Kit protocol, cDNA was synthesized from the obtained RNA.

Compound	Amount
Oligo (dT) 12-18	1 µL
RNA (1 ng -1 µg)	x µL
dNTP mix	1 µL
Sterile, distilled water	Fill up to 12 µL

The reaction mixture was heated for 5 minutes at 65°C, cooled down on ice and briefly centrifuged. 7 µL of the following master mix were added to each sample (modified from original protocol, since RNaseOUT is only needed if using less than 50 ng RNA).

Compound	Amount
5x First-strand buffer	4 µL
0.1 M DTT	2 µL
SuperScript II RT	1 µL

This mixture was incubated at 42°C for 50 minutes followed by 15 minutes at 70°C. Before using it for RT qPCR, the cDNA was diluted with ddH_2O (fill up to 200 µL).
For the RT qPCR, the following master mix was prepared:

Name	Description
KAPA SYBR® FAST qPCR Master Mix (2x) Universal	10 µL
FW & RV Primers (10 µM)	1 µL
ddH_2O	7 µL

For each sample, 18 µL of the master mix and 2 µL of the template DNA were mixed in a tube and the plate was subsequently centrifuged for 1 minute at 1500 rpm.

Then, the following PCR reaction was performed (on a Applied Biosystems 7500 Fast Real-Time PCR System using 7500 Software v2.3). For this experiment, the quantitation setting, which also calculates a comparative C_T ($\Delta\Delta C_T$), was used.

Initial denaturation	20'	95°C
40 cycles	3'	95°C
	30'	60°C
melting curve	15'	95°C
	1''	60°C
	15'	95°C
	15'	60°C

Microsoft Excel® for Mac 2011 (version 14.4.5) and GraphPad Prism 6 for Mac OS X (version 6.0d) were used for data analysis.

5. RESULTS

The following results show experimental analysis of our three candidate lncRNAs.

For *lncRNA-117* and *lncRNA-124*, the experiments were performed on homozygous *knockout* mice in comparison to age-matched littermate *wild type* (WT) mice under two different conditions: steady state or seven days post infection with ovalbumin-expressing *Listeria monocytogenes* (LM-OVA). The time point of seven days post infection was chosen, as it is at the peak of the immune response with increased formation of memory CD8 T cells while a large number of effector CD8 T cells is still present. This is of great importance for our research, since a preceding analysis showed that the two candidate lncRNAs are highly expressed in activated cytotoxic T cells and therefore, any defect in effector CD8 T cell differentiation, proliferation or cytotoxicity would become apparent.
Multiple experiments were performed under each condition. The mice had to reach a minimum age of 8 weeks before they were sacrificed. Depending on the focus of the experiment, cells were isolated from varying tissues, stained with fluorescent antibodies and subsequently analyzed using a BD FACS LSRII flow cytometer.

For the analysis of the *lncRNA-111* phenotype, only heterozygous knockout mice, which already showed a phenotype, were used for experimental analysis. They were not sacrificed and are currently being bred to generate homozygous knockout mice.

5.1 *IN VIVO* ANALYSIS OF *LNCRNA-117* KO MICE

5.1.1 Steady state analysis

The steady state analysis of *lncRNA-117* knockout mice and littermate wild type mice was performed at two separate times using 8 weeks old mice. To obtain a general overview of the impact of this lncRNA *in vivo*, we analyzed a variety of cell types in different organs.

Since the RNA-seq analysis by Christian Harman (see 3.2.3.A) showed high expression of *lncRNA-117* in natural killer T cells (NK T cells), the frequency of NK T cells was analyzed in wild type and knockout mice in three different organs and peripheral blood.

In Figure 5.1, the *lncRNA-117* knockout mice demonstrate a significant proportional increase of NK T cells in the pooled axial and brachial lymph nodes. However, the actual cell number in this organ shows solely a trend towards increased NK T cell counts in KOs. In peripheral blood samples, a significant increase of NK T cells in cell number and a slight trend in percentage were observed. Due to the low number of mice, the experiments will have to be repeated.

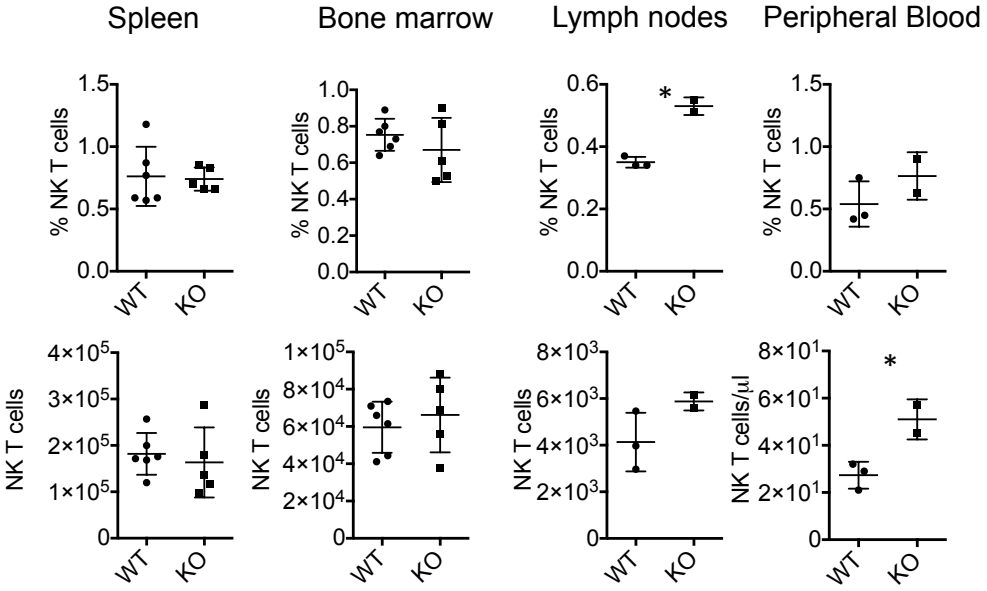

Figure 5.1 Steady state analyses of NK T cells

LncRNA-117 KO mice and littermate WT C57BL/6 mice were analyzed at the age of 8 weeks (two independent experiments). The staining for NK T cells was performed on cells of the spleen and bone marrow during both experiments (wild type n=6, lncRNA 117 knockout n=5), while it was only performed for the cells of the lymph nodes and peripheral blood (wild type n=3, lncRNA-117 knockout n = 2) during the second experiment. The percentage and cell numbers are depicted for all organs.

*The horizontal lines indicate the mean (and s.e.m.). * P < 0.05 (unpaired t-test).*

The analysis of $CD19^+$ B cells in the bone marrow and peripheral blood, but also in secondary lymphoid organs like spleen and lymph nodes, did not show any differences in percentage nor number between knockout and wild type mice during steady state (see Figure 5.2).

Subsequently, we analyzed the B1a subgroup, which showed high expression of our candidate lncRNA in Christian Harman's RNA-seq analysis. Using the already on

CD19^{+} gated B cells, we additionally gated on CD5^{+} expressing cells to analyze the percentage of B1a cells. We did not observe any significant differences between WT and *lncRNA-117* KO mice (data not shown).

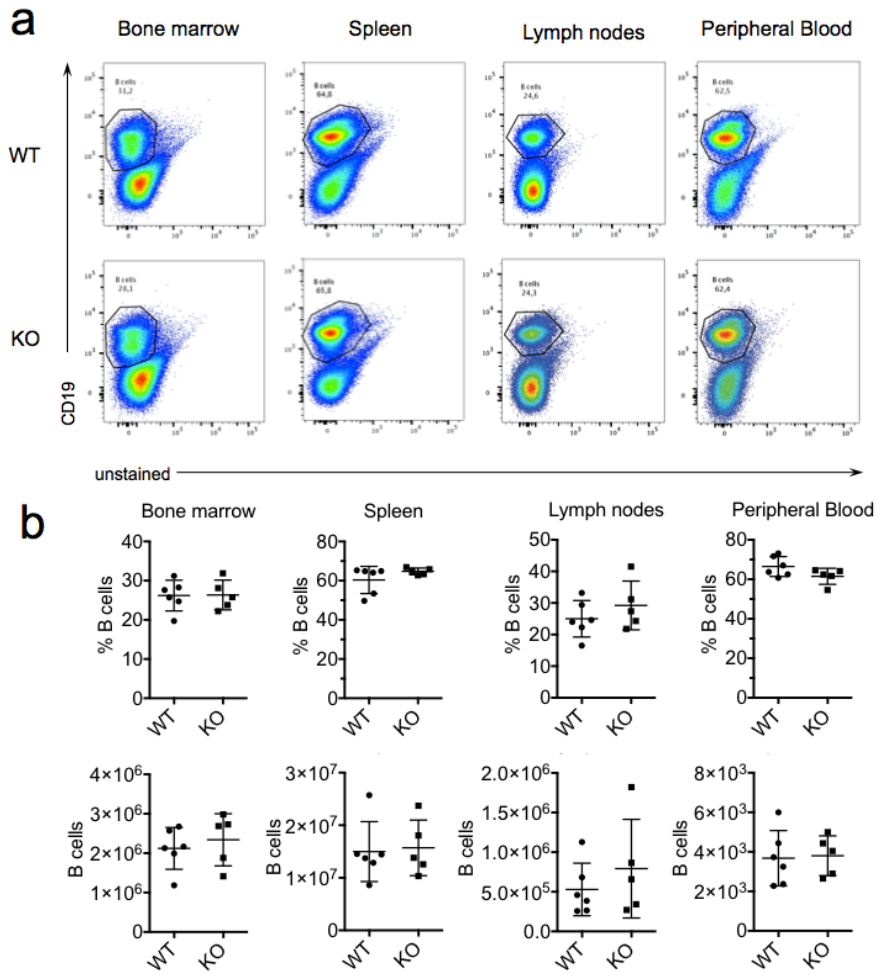

Figure 5.2 Frequency of B cells in various tissues during steady state

LncRNA-117 knockout mice (n=5) and littermate wild type C57BL/6 mice (n=6) were sacrificed at the age of 8 weeks. B cells were analyzed in the bone marrow, spleen, pooled axial and brachial lymph nodes and peripheral blood. The data was collected in two separate experiments.

(a) Representative FACS plots of B cell gating in wild type and knockout mice

(b) Percentage and number of B cells in wild type (WT) and lncRNA 117 knockout (KO) mice. The horizontal lines indicate the mean (and s.e.m.).

Following the analysis of B cells, we focused on the second major group of adaptive immune cells, the T cells. The RNA-seq analysis revealed an elevated expression of *lncRNA-117* in activated CD8 T cells as well as in one major T helper subset, the T_H1 cells. Therefore, we performed a broad analysis examining the cell numbers, the CD8:CD4 ratio and the percentage of naïve, central memory and effector memory CD8 and CD4 T cells in the spleen, lung and lymph nodes.

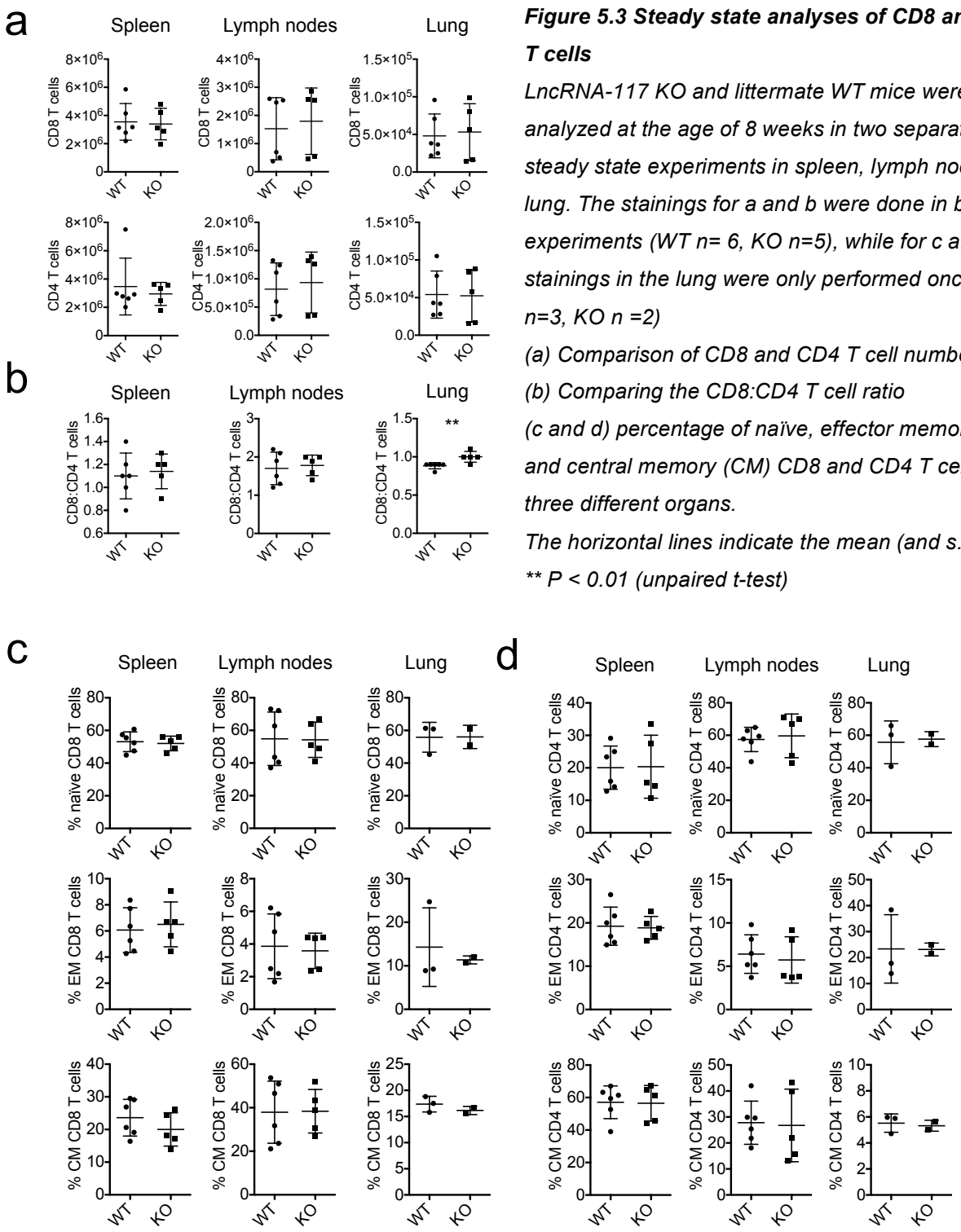

Figure 5.3 Steady state analyses of CD8 and CD4 T cells

LncRNA-117 KO and littermate WT mice were analyzed at the age of 8 weeks in two separate steady state experiments in spleen, lymph nodes and lung. The stainings for a and b were done in both experiments (WT n= 6, KO n=5), while for c and d the stainings in the lung were only performed once (WT n=3, KO n =2)

(a) Comparison of CD8 and CD4 T cell numbers

(b) Comparing the CD8:CD4 T cell ratio

(c and d) percentage of naïve, effector memory (EM) and central memory (CM) CD8 and CD4 T cells in three different organs.

The horizontal lines indicate the mean (and s.e.m.).

*** P < 0.01 (unpaired t-test)*

The CD8:CD4 ratio in the lung shows a significant change in composition when comparing *lncRNA-117* knockout and wild type mice. No difference was observed in the spleen and lymph nodes. The knockout of *lncRNA-117* did not affect CD4 and CD8 T cell numbers nor the percentage of naïve, effector memory and central memory T cells during steady state.

During the second steady state experiment, antibodies for CXCR3 were used to gate on T_H1 cells in CD4 T cells. The results showed no difference in percentage or number between KO and WT mice (data not shown).

We also analyzed the T cell development in the thymus by analyzing the number of thymocytes and the percentage of double negative (DN), double positive (DP), CD8 single positive and CD4 single positive T cells. We observed no significant difference in the development of thymocytes between WT and *lncRNA-117* KO mice.

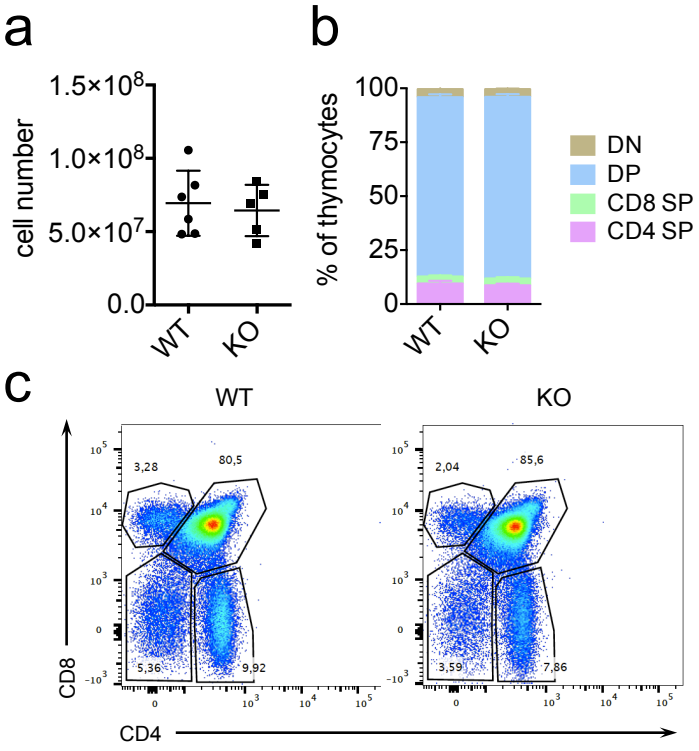

Figure 5.4 Steady state analysis of thymocytes

The thymuses of lncRNA-117 knockout mice (n=5) and littermate wild type mice (n=6) were analyzed at the age of 8 weeks (steady state).

(a) Analysis of the total cell number in the thymus

(b) Analysis of the distribution of double negative (DN), double positive (DP), CD8 single positive (CD8 SP) and CD4 single positive (CD4 SP) T cells.

(c) Representative flow cytometry plots of the gating strategy used for the four cell types in both mouse strains.

The horizontal lines indicate the mean (and s.e.m.).

To examine if there was any disparity in effector functions of T cells, splenocytes were stimulated with Phorbol 12-myristate 13-acetate (PMA) and Ionomycin for 4.5 hours in the presence of Brefeldin A (BFA) and subsequently analyzed for their Interferon γ (IFN γ) production.

The preliminary data obtained from a small cohort of mice shows a significant decrease in the production of IFN γ by activated CD8 T cells in knockout mice as well as a trend for less IFN γ production in activated CD4 T cells.

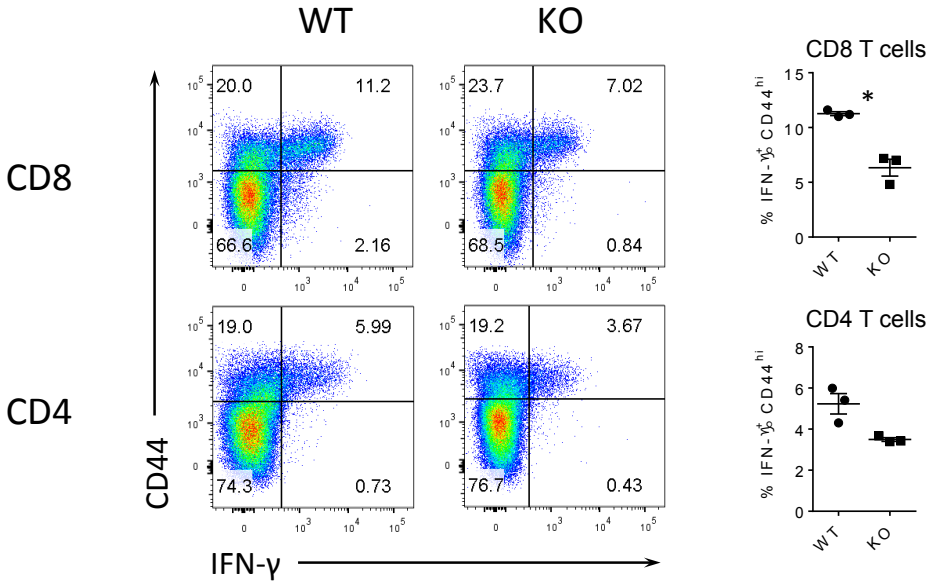

Figure 5.5 Steady state analysis of IFNγ production in CD44^{hi} T cells

The steady state analysis shows splenocytes from wild type (n=3) and lncRNA-117 knockout (n=3) littermates at the age of 8 weeks. The splenocytes were stimulated for 4.5h with PMA and Ionomycin in the presence of BFA and subsequently analyzed. The cells were first gated on either CD4^{+} or CD8^{+} T cells.

*The horizontal lines indicate the mean (and s.e.m.). * P < 0.05 (unpaired t-test).*

Except for the above-mentioned results no difference was observed between wild type and knockout mice regarding the CD8 and CD4 T cell counts in the bone marrow and peripheral blood as well as lymphocyte count in lung and peripheral blood. Additionally, the frequency of natural killer cells was not altered in the *lncRNA-117* KO mice. The cell count of macrophages and dendritic cells was also determined in the spleen and bone marrow, but no difference could be detected. Also, a hemogram was performed on the blood sample of each mouse using HemaTrue Hematology Analyzer, which did not show any significant differences (data not shown).

5.1.2 Post infection analysis

Since *lncRNA-117* is highly expressed in effector and memory CD8 T cells, age-matched *lncRNA-117* knockout and wild type mice were infected in two separate experiments intravenously (i.v.) with ovalbumin-expressing *Listeria monocytogenes* (LM-OVA). This infection model was used to analyze the role of *lncRNA-117* in effector T cell proliferation, differentiation and function *in vivo*.

The analysis of cells in the secondary lymphoid organs (lymph nodes and spleen) showed that knockout mice (n=5) had an overall decrease in cell number, which was also observed in the subgroups, in the pooled axial and brachial lymph nodes in comparison to wild type mice (n=7). This result was not observed in the spleen.

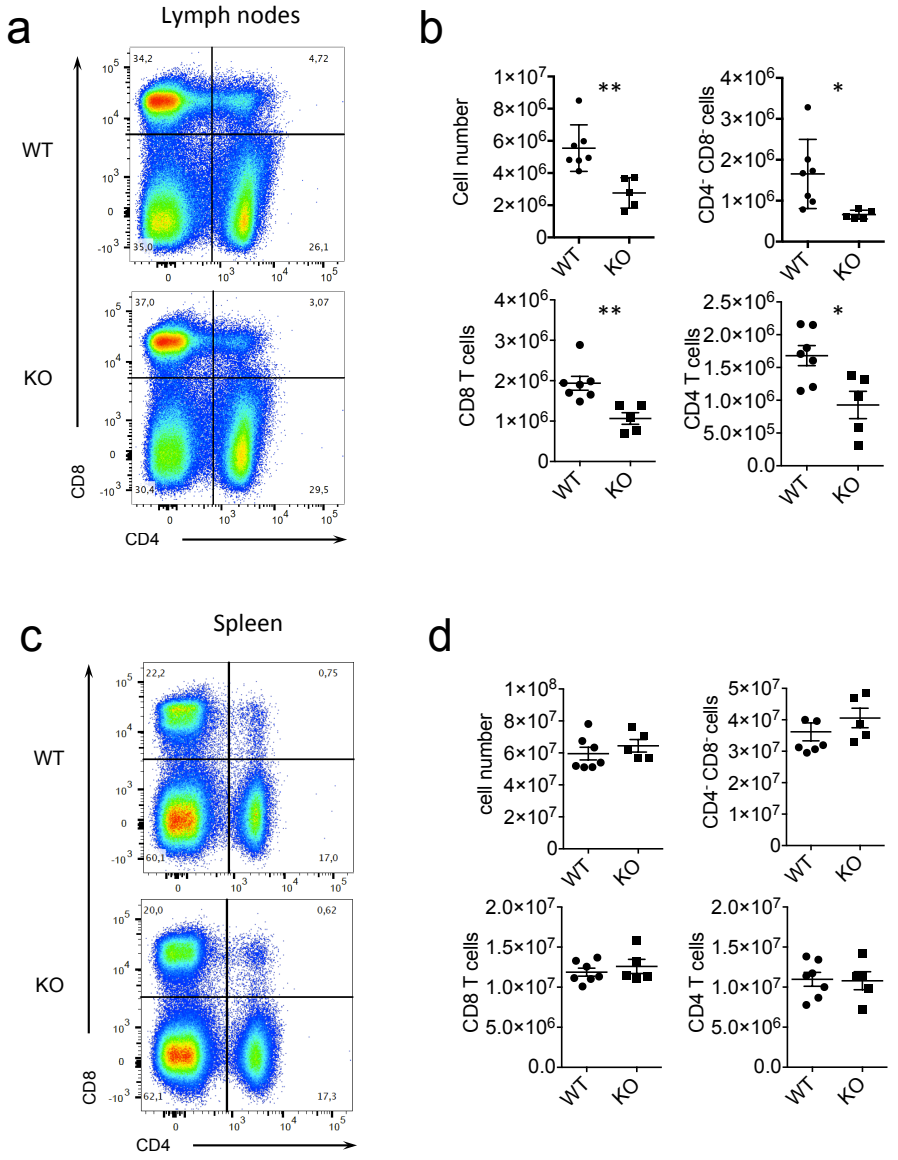

Figure 5.6 Analysis of the lymph nodes seven days post infection with Listeria monocytogenes

Wild type (n=7) and lncRNA-117 knockout (n=5) littermates were infected i.v. with 1x 10^5 LM-OVA. Seven days post infection, the T cells of the lymph nodes (axial and brachial) and the spleen were analyzed.

(a and c) Representative flow cytometry plots showing CD4 and CD8 T cells from WT and lncRNA-117 KO mice.

(b and d) Analysis of (b) the lymph nodes and (d) the spleen showing total lymphocytes, the number of double negative cells (including B cells), CD8 T cells and CD4 T cells in WT and KO mice.

The horizontal lines indicate the mean (and s.e.m.).

** P < 0.05 (unpaired t-test).*

*** P < 0.01 (unpaired t-test).*

In addition, CD8 and CD4 T cell counts were also calculated for the lung, which, like the spleen, did not show any differences between WT and KO mice (data not shown).

Stimulated splenocytes taken from a small cohort of mice showed increased degranulation in CD8 T cells of *lncRNA-117* knockout (n=2) compared to WT (n=2) mice. Degranulation was measured by flow cytometry and by determining the expression of the degranulation surface marker CD107a on $CD44^{hi}$ effector/memory CD4 and CD8 T cells. For CD4 T cells, only a tendency for increased degranulation was observed. To make a clear statement, this experiment will have to be repeated with a larger number of WT and *lncRNA-117* KO mice.

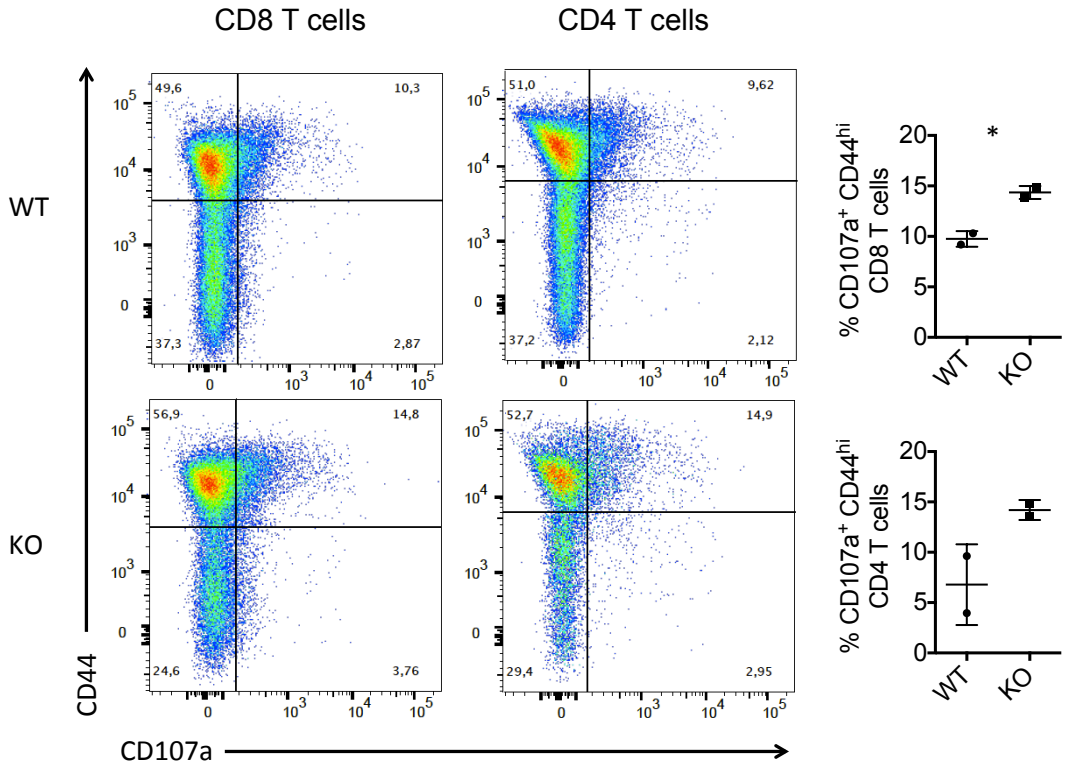

Figure 5.7 Analysis of $CD44^{hi}$ $CD107a^{+}$ splenocytes after re-stimulation in vitro

Wild type (n=2) and lncRNA-117 knockout (n=2) littermates were infected i.v. with 1x 10^5 LM-OVA. After seven days, the spleen was extracted and splenocytes of wild type and knockout mice were separately stimulated for 4.5h with PMA and Ionomycin in the presence of BFA. Representative flow cytometry plots for $CD44^{hi}$ $CD107^{+}$ CD8 and CD4 T cells and the analyzed percentage of each are shown.

*The horizontal lines indicate the mean (and s.e.m.). * P < 0.05 (unpaired t-test).*

Our previous experiment under steady state condition, which indicated decreased IFN γ production in CD8 T cells (see Figure 5.5), was repeated under post infection conditions with a small cohort of mice. However, our analysis rather showed an increase in IFN γ production. For clarification purposes, this experiment will have to be repeated with a larger number of mice.

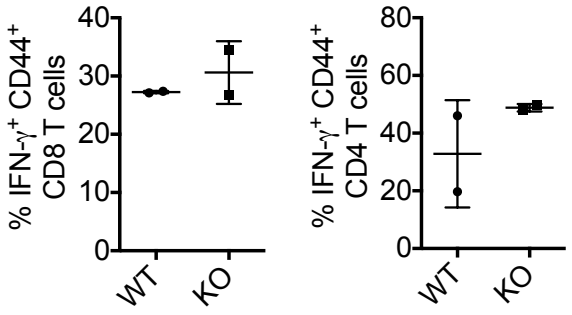

Figure 5.8 Analysis of IFNγ^{+} CD44^{hi} splenocytes after re-stimulation in vitro

Wild type (n=2) and lncRNA-117 knockout (n=2) littermates were infected i.v. with 1x 10^5 LM-OVA. After seven days, the spleen was extracted and splenocytes of wild type and knockout mice were stimulated for 4.5h with PMA and Ionomycin. The percentage of IFN γ positive activated T cells is shown in two graphs.

The horizontal lines indicate the mean (and s.e.m.).

Other stainings were performed as well, whose analyses are not shown here due to their consistently negative outcome: In spleen and lung, the percentages/numbers of naïve, effector memory, central memory and KLRG1^{+}- CD8 T cells were analyzed and the results were not different between knockout and wild type littermates (data not shown). As shown in steady state experiments, blood samples were also analyzed with the HemaTrue Hematology Analyzer and showed no significant differences.

5.2 *IN VIVO* ANALYSIS OF *LNCRNA-124* KO MICE

5.2.1 Steady state analysis

For the analysis of *lncRNA-124*, the same experimental set up was used as for *lncRNA-117* during steady state: Littermate knockout and wild type mice were sacrificed at a minimum age of 8 weeks in 2 separate experiments, and multiple cell types from different organs were analyzed.

The CD4 and CD8 T cell numbers were compared between wild type and knockout mice in 4 different organs: spleen, pooled axial and brachial lymph nodes, bone marrow and peripheral blood. First, the cells were gated on lymphocytes, then on αβ T cells by gating on TCR β positive cells and, finally, gating on CD4 and CD8 T cell subsets (Figure 5.9 b).

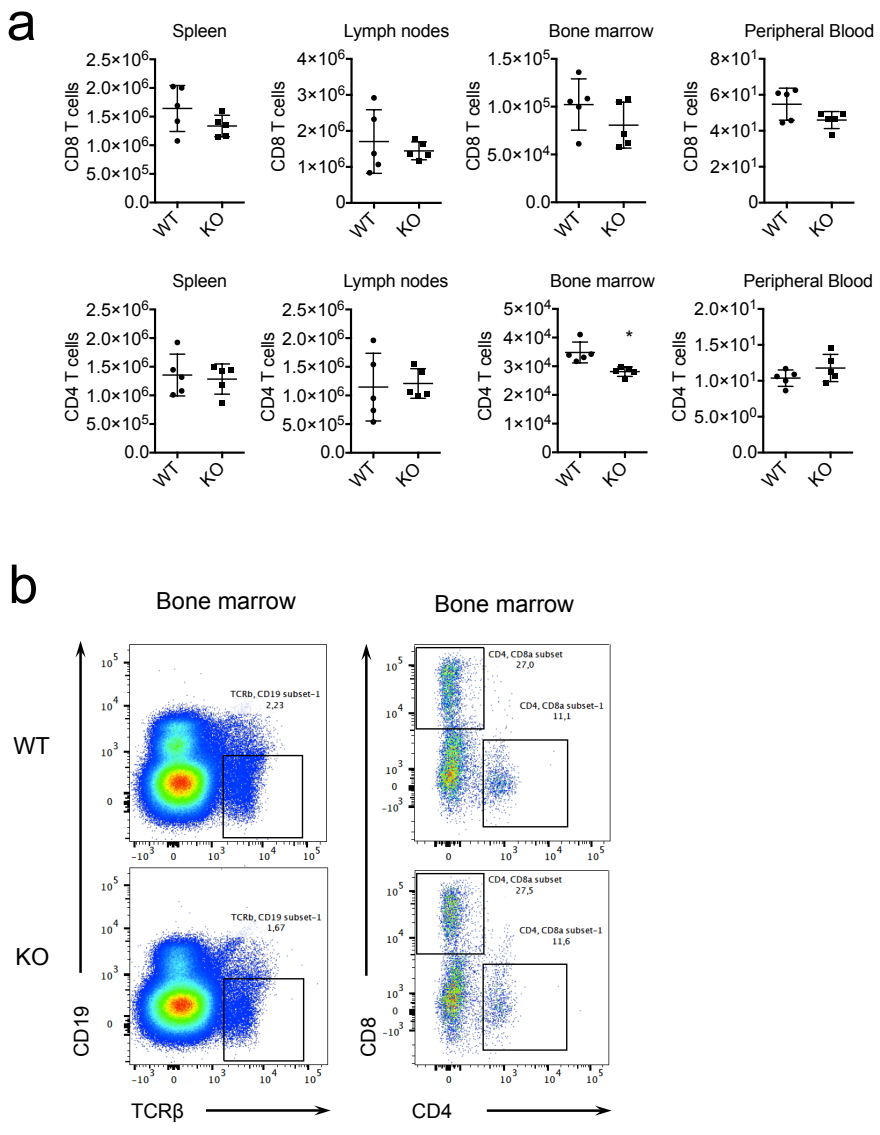

Figure 5.9 Steady state analyses of CD4 and CD8 T cells in different organs

The CD8 and CD4 T cells of lncRNA-124 knockout (n=5) and wild type littermate (n=5) mice were analyzed at the age of 8 weeks.

(a) Comparison of CD8 and CD4 T cell numbers in the spleen, pooled axial and brachial lymph nodes, bone marrow and peripheral blood.

(b) Representative flow cytometry plots showing the gating for all T cells and subsequently for CD4 or CD8 T cells in the bone marrow.

The horizontal lines indicate the mean (and s.e.m.).

** P < 0.05 (unpaired t-test).*

Only CD4 T cells in the bone marrow showed a significant decrease in *lncRNA-124* knockout mice in comparison to their wild type littermates, while there seems to be no significant change in any other organ.

Since we only have confined knowledge about the expression patterns of *lncRNA-124*, we also tested if the knockout had an impact on tissue-resident T cells in the two organs most prominent for them: the lung and the small intestine. To identify tissue-resident CD4 and CD8 T cells, we determined the percentage of cells expressing CD69 and CD103, two markers that have been shown to identify tissue-resident T cells. The *lncRNA-124* knockout seems to have no effect on either CD4 or CD8 tissue-resident T cell.

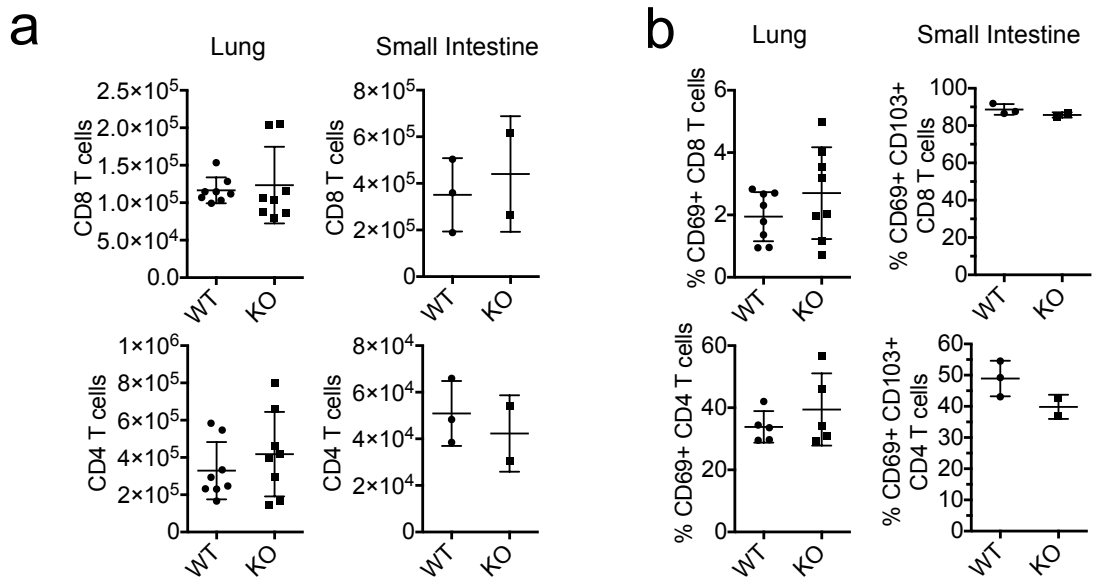

Figure 5.10 Steady state analysis of tissue-resident T cells

LncRNA-124 knockout (KO) and wild type (WT) littermate mice were analyzed at the age of 8 weeks. The lung (KO n= 8, WT n=8) and small intestine (KO n=2, WT n=3) were used for analysis of tissue resident T cells.

(a) CD8 and CD4 T cell numbers in the lung and the small intestine.

(b) Percentage of CD8 and CD4 tissue-resident T cells in the lung and the small intestine expressing CD69 and CD103.

The horizontal lines indicate the mean (and s.e.m.).

According to the qPCR, which showed a high expression of the candidate lncRNA in the thymus, we analyzed T cell development of *lncRNA-124* KO mice. This was done by staining for double negative (DN), double positive (DP), CD4 and CD8 single positive T cells. Our analysis did not reveal any significant role of *lncRNA-124* in T cell development in the thymus.

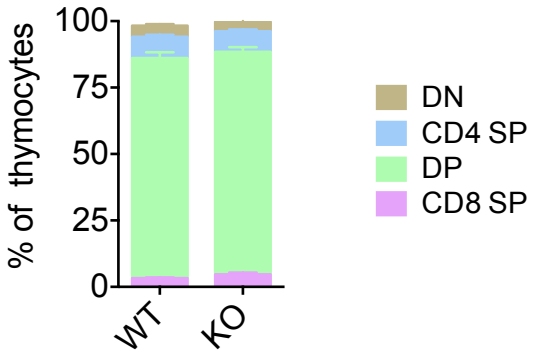

Figure 5.11 Steady state analysis of thymocytes

The thymocytes of lncRNA-124 knockout and wild type littermate mice were analyzed at the age of 8 weeks.

The distribution of thymocytes, comparing double negative (DN), double positive (DP), CD8 single positive (CD8 SP) and CD4 single positive (CD4 SP) T cells between both mouse strains are shown in this graph.

During steady state, we also observed that *lncRNA-124* KO mice did not show any difference in the number of NK cells, NK T cells and B cells in the spleen, lymph nodes, bone marrow and peripheral blood. In addition, the proportion of naïve, effector memory and central memory CD8 T cells was similar between WT and KO mice.

After stimulation of splenocytes with PMA and Ionomycin, no significant changes in the degranulation or production of IFN γ were observed in CD8 and CD4 T cells. As in *lncRNA-117* knockout mice, the blood count was also analyzed in *lncRNA-124* knockout mice using the HemaTrue Hematology Analyzer, which showed no significant differences between knockout and wild type blood samples (data not shown).

5.2.2 Post infection analysis

Since *lncRNA-124* was highly expressed in effector CD8 T cells isolated from the spleen of mice seven days post infection with LM-OVA, we analyzed whether fully functional effector CD8 T cells would be generated in *lncRNA-124* KO mice following infection with LM-OVA.

Splenocytes were chosen for the analysis of T cell activation, because the spleen is the major source of T cells and one of the major target organs of LM-OVA replication.

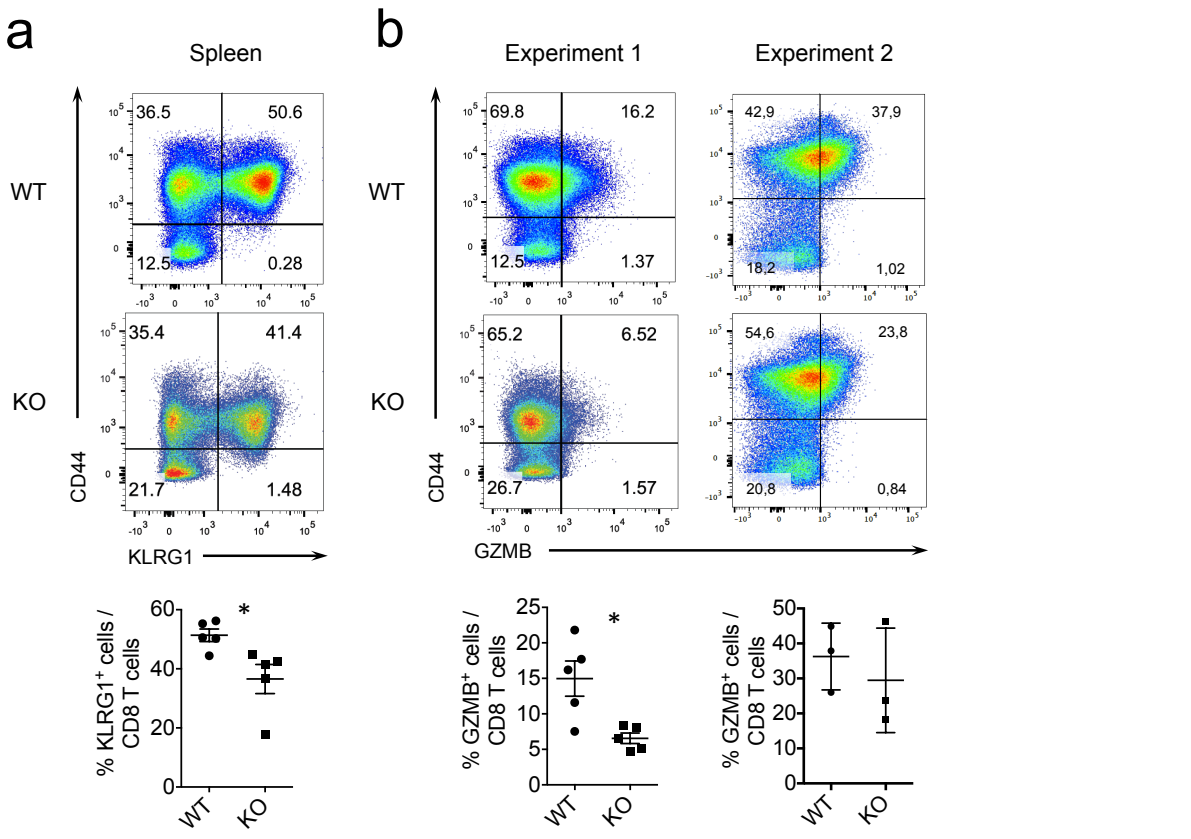

Figure 5.12 Analysis of KLRG1 expression and granzyme B production of CD8 T cells seven days post infection with Listeria monocytogenes

The CD8 T cells of lncRNA-124 knockout mice and littermate wild type mice were analyzed in two separate experiments (exp. 1: n=10; exp. 2: n= 6) seven days after infection with 1x 10^5 LM-OVA.

(a) Representative flow cytometry plots and percentage of KLRG1$^+$ CD8 T cells in the spleen of the first experiment

(b) Representative flow cytometry plots and percentage of two experiments comparing the granzyme B production in activated T cells

*The horizontal lines indicate the mean (and s.e.m.). * P < 0.05 (unpaired t-test).*

In the first experiment (Figure 5.12 a and b), the knockout mice (n=5) show a significant lower percentage of KLRG1$^+$ CD8 T cells as well as granzyme B producing CD8 T cells in comparison to wild type mice (n=5). Since the overall expression of granzyme B was higher in the second experiment, we were not able to combine the results from both experiments. Further experiments will be needed to verify whether *lncRNA-124* affects granzyme B expression in CD8 T cells.

We also analyzed the activation of CD4 T cells, in particular T_H1 T cells, in the spleen. Therefore, we used CD44 as a marker for T cell activation/maturation and CXCR3 as a marker for T_H1 maturation. In this experiment, *lncRNA-124* knockouts (n=4) showed a significant increase in CXCR3$^-$ CD44$^-$ CD4 T cells while there was a decrease in CXCR3$^+$ CD44$^+$ CD4 cells in comparison to wild type mice (n=4).

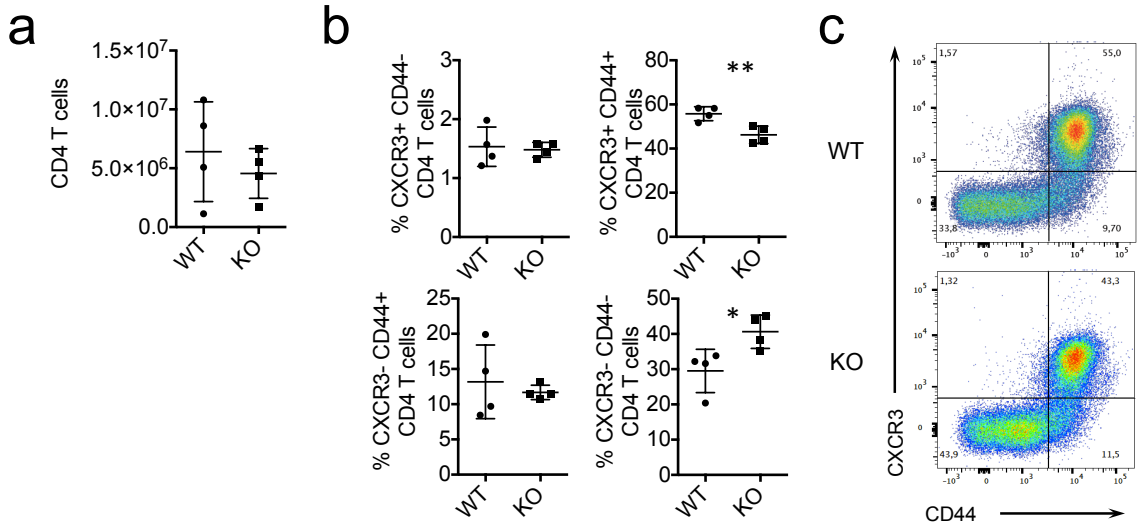

Figure 5.13 T_H1 cells are decreased in the spleen of lncRNA-124 KO mice following LM-OVA infection

The expression of CXCR3 was analyzed in CD4 T cells of the spleen of lncRNA-124 knockout (n=4) and littermate wild type (n=4) mice seven days post infection with 1x 10^5 LM-OVA.

(a) Calculated number of CD4 T cells in the spleen.

(b) Graphs showing percentage of CD4 T cells expressing one of the following four combinations of CXCR3 and CD44: CXCR3$^+$ CD44$^-$, CXCR3$^+$ CD44$^+$, CXCR3$^-$ CD44$^+$ and CXCR3$^-$ CD44$^-$.

(c) Representative flow cytometry plots of wild type (WT) and knockout (KO) splenocytes, first gated on CD4 T cells and then relative to the CXCR3 and CD44 expression.

The horizontal lines indicate the mean (and s.e.m.).

** P < 0.05 (unpaired t-test). ** P < 0.01 (unpaired t-test).*

In addition, we analyzed the degranulation potential and cytokine production of activated T cells. Therefore, splenocytes were stimulated for 4.5 hours with PMA and Ionomycin and subsequently stained for IFN γ as well as the degranulation marker CD107a in CD4 and CD8 T cells. Comparing the percentage of both markers in these cell types showed no difference between wild type and *lncRNA-124* knockout mice.

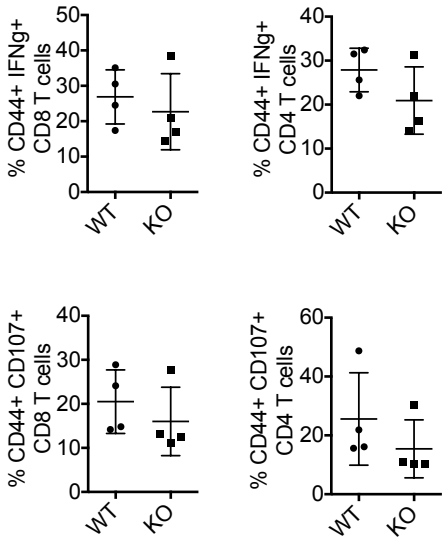

Figure 5.14 Post infection analysis of IFNγ production and granules release of CD8 and CD4 T cells after re-stimulation

Seven days post infection with 1x 10^5 Listeria monocytogenes, the splenocytes of lncRNA-124 knockout mice (n=4) and littermate wild type mice (n=4) were stimulated for 4.5 hours with PMA and Ionomycin. Here, the percentage of activated CD8 and CD4 T cells producing Interferon γ (IFN γ) and their degranulation capacity (CD107a) are shown.

The horizontal lines indicate the mean (and s.e.m.).

Samples from peripheral blood, lymph nodes and spleen were analyzed regarding CD8 T cell counts as well as the percentage of naïve, effector and central memory cytotoxic T cells. There are two reasons for this analysis: First, we wanted to see if the lack of *lncRNA-124* expression had any impact on the generation of effector T cells. Second, since this candidate lncRNA is located next to *Id2*, which is important for effector memory CD8 T cell survival and memory cell formation, a possible interaction between those two genes could be determined by an altered T_{EM} cell count in knockouts[36]. While neither the total cytotoxic T cell counts nor the naïve and especially the effector CD8 T cell numbers showed any differences between wild type (n=4) and knockout (n=4) mice, the formation of central memory cells was significantly increased in *lncRNA-124* knockout mice.

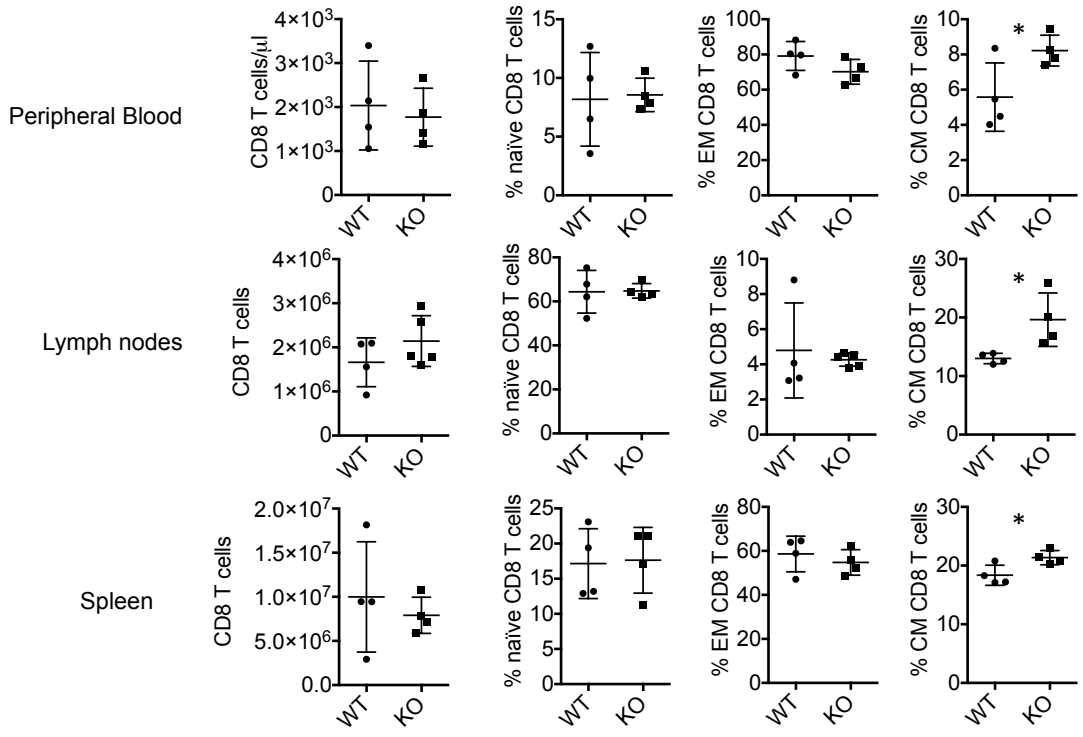

Figure 5.15 Post infection analysis of CD8 T cell subsets

Seven days post infection with 1x 10^5 Listeria monocytogenes, the CD8 T cell numbers as well as the percentage of the naïve CD8, effector memory (EM) CD8 and central memory (CM) CD8 T cells were analyzed in lncRNA-124 knockout (n=4) and littermate wild type (n= 4) mice. This analysis was performed in the peripheral blood, in the axial and brachial lymph nodes and spleen.

*The horizontal lines indicate the mean (and s.e.m.). * P < 0.05 (unpaired t-test).*

Further analysis of *lncRNA-124* knockout mice showed that CD4 and CD8 naïve, effector memory and central memory cells in the lung were not affected. In addition, the frequency of tissue-resident CD4 T cells did not show any difference between WT and KO mice.

Blood samples from *lncRNA-124* knockout and WT mice were analyzed on the HemaTrue Hematology Analyzer. The results showed no significant differences of the analyzed cell counts (data not shown).

5.3 PHENOTYPE OF *LNCRNA-111* KO MICE

Even though the breeding of *lncRNA-111* knockout mice has not yet resulted in homozygous mice, germline heterozygous mice displayed bilateral microphthalmia possibly caused by an inflammatory condition. Mice that were genotyped positive for the knockout were easily distinguished from their wild type littermates by means of the phenotype as early as 2 to 3 weeks after date of birth.

We treated the eyes of the *lncRNA-111* heterozygous mice for three consecutive weeks with an anti-inflammatory ophthalmic ointment, which moderately improved the microphthalmia. The pictures depicted in Figure 5.16 show the mice at the end of the treatment in comparison to one wild type littermate mouse.

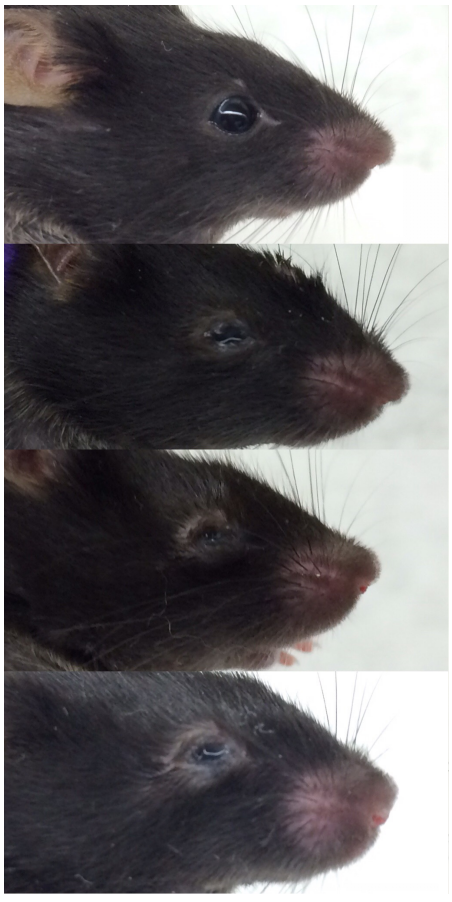

Figure 5.16 LncRNA-111 heterozygous knockout mice after treatment with antibacterial ointment
LncRNA-111 heterozygous knockout mice were treated for three weeks with sterile ophthalmic ointment. The top picture shows the right eye of an untreated male wild type littermate, while the following three pictures depict the right eyes of three male heterozygous knockout mice after the treatment.

Since we did not want to sacrifice any mice at this time point, we could not do any microscopic analysis of the microphthalmia phenotype of the eye.

However, I performed an online research of genes known to cause microphthalmia in humans (using www.omim.org) and of their homologous genes in mice. These genes and their location are listed in Table 5.17.

Human gene	human Chr.	homolog mouse gene	mouse Chr	
MCOPCT1	16p13.3	?	?	
MCOPCB1	Chr. X	?	?	
MCOPCB2	15q12-q15	?	?	
MCOPCB3 (MCOP2 CHX10, HOX10)	14q24.3	Vsx2	Chr 12	Visual system homeobox 2
MCOPCB4	?	?	?	
MCOPCB5 (SHH, HPE3, HLP3, SMMCI)	7q36.3	SHH	Chr 5	Sonic hedgehog
MCOPCB6	8q22.1	Gdf6	Chr 4	Growth differentiation factor 6
	12p13.31	Gdf3	Chr 6	Vgr2, ecat9
MCOPCB9	4q35.1	TENM3	Chr 8	teneurin transmembrane protein 3
MCOP1	14q32	?	?	
MCOP2	see MCOPCB3			
MCOP3 (RAX, RX)	18q21.32	Rax	Chr18	retina and anterior neural fold homeobox
MCOP4 (MCOPCB6, GDF6, KFS1, LCA17)	8q22.1	Gdf6	see Gdf6	
MCOP5 (MFRP, NNO2)	11q23.3	Mfrp	Chr9	membrane frizzled-related protein
MCOP6 (PRSS56)	2q37.1	Prss56	Chr1	protease, serine 56
MCOP7 (GDF3, KFS3, MCOPCB6)	see MCOPCB6			
MCOP8 (ALDH1A3, ALDH6)	15q26.3	Aldh1a3	Chr 7	aldehyde dehydrogenase family 1, subfamily A3
ODRMD (Six6)	14q23.1	Six6	Chr12	sine oxulis-related homeobox 6

Table 5.17 Analysis of microphthalmia-related genes in humans and mice

The table shows the names of the human genes related to microphthalmia and their chromosomal coordinates, the names of homologous mouse genes, their location and their full names.

A question mark signals that either the location or the mouse equivalent for the human gene has not been discovered yet or does not exist.

The gene-based research showed that none of the homologous mouse genes were located on the same chromosome as *lncRNA-111*. This observation does not mean that the phenotype could not be associated with microphthalmia: First, long non-coding RNAs can also interact with genes or their products in trans. Second, since microphthalmia is rare, the lncRNA could interact with a gene, which is not yet known to cause this disease.

6. DISCUSSION

6.1 *LncRNA-117*$^{-/-}$ AND *LncRNA-124*$^{-/-}$ *MICE*

In an effort to identify lncRNAs that regulate CD8 T cell function and differentiation, we performed deep RNA-seq of CD8 T cell subsets generated *in vivo* following *Listeria monocytogenes* infection. From two promising candidates, *lncRNA-117* and *lncRNA-124*, which are both upregulated in effector CD8 T cells, KO mice were generated using CRISPR/Cas9-mediated genome engineering. Our results indicate that *lncRNA-117* may affect cytotoxicity as well as lymphocyte numbers in the peripheral lymph nodes at day seven post infection with *Listeria monocytogenes*. *LncRNA-124* does not seem to regulate its neighboring gene *Id2*, but instead affects central memory CD8 T cell formation.

6.1.1 The impact of *lncRNA-117* and *lncRNA-124* on immune cells

Although we used an *in vivo* model to study the role of lncRNAs in CD8 T cell differentiation and memory formation, we were also interested whether *lncRNA-117* and *lncRNA-124* may influence other immune cells.

Computational analysis of published RNA-seq data, performed by Christian Harman, revealed that *lncRNA-117* is also highly expressed in B cells, T_H1 cells and natural killer T (NKT) cells. Our analysis of *lncRNA-117*$^{-/-}$ mice at steady state indicates that *lncRNA-117* does not influence B cell and CD4 T cell subsets (see Figures 5.2 and 5.3). However, the percentage of IFN-γ-producing CD4 T cells may be decreased in *lncRNA-117* KO mice. As this was only one experiment with three mice per group, and the result was not statistically significant, this experiment has to be repeated. While NKT cells seemed to be present in significantly higher amounts in the lymph nodes and blood of *lncRNA-117* KO mice during steady state (see Figure 5.1), the number of mice was too small to draw any conclusions yet. Further experiments will be necessary to determine whether the knockout of *lncRNA-117* does regulate the NKT cell development or survival.

Due to the fact that *lncRNA-124* is not annotated in any public databases, we do not have any additional information about the expression levels in other cell types. We chose to analyze NK cells, NKT cells, B cells and CD4 T cells in *lncRNA-124* KO mice. At steady state, the number of those cells did not show any changes in a

variety of organs, except for a significant decrease of CD4 T cells solely observed in the bone marrow (see Figure 5.9).
As we performed an analysis of CD4 T cells in the spleen following LM-OVA infection, the overall CD4 T cell number showed no significant difference between KO and WT mice. Since *Listeria* initiates a strong T_H1 cell response, we analyzed the composition of CD4 T cells, which showed a significant proportional decrease of activated T_H1 cells and an increase in $CD44^-$ $CXCR3^-$ CD4 T cells in the KO mice (see Figure 5.13)[1]. This experiment will have to be repeated to make a clear statement. If the *lncRNA-124* knockout impairs the activation of T_H1 cells, the decreased quantity could also cause a reduction in the activation of macrophages and CD8 T cells and subsequently a weakened immune response[56].

6.1.2 The roles of *lncRNA-117* and *lncRNA-124* during infection

Our RNA-seq analysis showed that the *lncRNA-117* and *lncRNA-124* were low expressed in naïve CD8 T cells and highly expressed in SLECs, MPECs and memory CD8 T cells. Therefore, it is possible that the lncRNAs have an impact on the effector functions of T cells, as has been shown for the lncRNA *NeST*, which regulates IFN γ production in CD8 T cells[26].

Seven days post infection, we analyzed IFN γ as well as the degranulation molecule CD107a, which is a measure of cytotoxicity. *In vitro* re-stimulation of CD8 T cells extracted from *lncRNA-117* KO mice showed that a higher percentage of CD8 T cells expressed the degranulation marker CD107a while IFN-γ production was not affected (see Figures 5.7 and 5.8). Due to the limited number of mice, these experiments have to be repeated first before any conclusions can be made. Currently, it is also unclear how *lncRNA-117* may regulate cytotoxicity and whether this may affect the bacterial load in the spleen and liver of *Listeria monocytogenes*-infected KO mice. However, no difference in mortality has been observed until seven days post infection with *Listeria monocytogenes*.

When we analyzed degranulation markers and IFN γ in *lncRNA-124* KO mice after *in vitro* re-stimulation, we observed no significant difference between WT and KO mice. The results for granzyme B (GZMB) production turned out to be contradictory: On the one hand, the two performed experiments could not be merged due to incomparable

percentages of cells expressing GZMB, and on the other hand, the first experiment showed significantly decreased GZMB production in KO mice while the second experiment did not. A possible explanation for the decreased production of GZMB in the first experiment could be the low amount of KLRG1^{+} CD8 T cells in these mice. To make a clear statement, this experiment will have to be repeated.

6.1.3 The lymph node phenotype of *lncRNA-117* KO mice

The post infection experiments showed that the cell number in the pooled axial and brachial lymph nodes of *lncRNA-117* KO mice was significantly lower than in WT mice. The significant reduction can be seen in CD8 T cell, CD4 T cell and B cell numbers. The same analysis was also performed for the spleen, where we did not see any difference in cell numbers.
Whether the lower cell numbers in the lymph nodes of *lncRNA-124* KO mice are due to decreased migration to or expansion of immune cells in the lymph node has yet to be determined.

6.1.4 The central memory CD8 T cell phenotype in *lncRNA-124 KO mice*

As mentioned in 3.2.3.B, *Id2* is the closest protein-coding neighboring gene of *lncRNA-124*: In *Id2*-deficient mice it has been shown that effector memory (EM) CD8 T cells are highly susceptible to apoptosis, which consequently leads to a significant reduction of this subset. Yet, central memory (CM) CD8 T cells showed no significant change in percentage or number[36]. If *lncRNA-124* would interact with *Id2*, which was hypothesized due to its proximity, we would have expected a similar outcome in *lncRNA-124*-deficient mice.
Therefore, we analyzed naïve, effector memory and central memory CD8 T cells seven days post infection with LM-OVA in *lncRNA-124* KO mice. The analysis of our experiments showed no change in the percentage of EM CD8 T cells, while CM CD8 T cells were proportionally elevated in the peripheral blood, lymph nodes and spleen of *lncRNA-124* KO mice. This result led to the rejection of the hypothesis that *lncRNA-124* interacts with *Id2*. However, we propose the new hypothesis that *lncRNA-124* could play a role in the conversion of effector to memory CD8 T cells.

6.1.5 Challenges and Outlook

The results obtained from *lncRNA-117* and *lncRNA-124* KO mice can be seen as preliminary. It is known that T cells have specific TCRs, which do not interact with every pathogen. Considering this, even small changes observed in our analysis could turn out to be significant if we repeat the experiment focusing only on the OVA-specific T cells. Therefore, we already started breeding the lncRNA KO mice with $RAG2^{-/-}$ OT-I TCR-transgenic mice. The offspring will only have OVA-specific adaptive immune cells of which we will sort the naïve OT-I cells for adoptive transfer into *C57BL/6* mice. We will repeat the infection experiments and analyze the generation of effector and memory CD8 T cell subsets. In addition, this experimental set-up allows us to analyze the role of the lncRNAs on solely CD8 T cell, which will simplify the interpretation of the results.

However, the performed experiments were not only essential to make first assumptions regarding the role of lncRNAs: Lab internal experiments by Christian Harman and Will Bailis showed the importance of comparing lncRNA KO mice with littermate WT mice, as minor genetic differences between mouse substrains, the gut microbiota and other factors can alter the phenotype and lead to inaccurate interpretations.

The study of these lncRNAs could eventually lead to the discovery of new regulatory networks or new players, which may play an important role in infections, autoimmunity, allergies or chronic inflammation.

6.2 *LNCRNA-111*$^{+/-}$ MICE

The main goal of this study was to find a possible explanation for the severe eye phenotype observed in heterozygous *lncRNA-111* KO mice without sacrificing them. As we know, the candidate lncRNA is not only highly expressed in naïve and memory CD8 T cells, but also in the retinal pigment epithelium (RPE; see 3.2.3.C).
The observation of the eye phenotype led us to research existing knowledge about the RPE: It plays an important role in the immune privilege of the eye, as it is not only an essential part of the blood-retinal barrier, but can also inhibit T cells and induce the commitment of CD4 T cells to the T_{reg} cell lineage[57,58]. The inhibitory functions of the RPE on cytotoxic T cells, which inhibits proliferation and secretion of inflammatory cytokines, could be impaired in the KO mice and therefore allow cytotoxic T cells to maintain active and to cause damage/inflammation to the eye[59]. Additionally, due to the ocular immune privilege, T cells cannot establish peripheral tolerance against specific eye antigens[60]. Therefore, in the case of an impaired immune privilege, not only pathogens and the following immune response against them, but also "autoreactive" T cells can cause significant damage to the eye.

As our experiment showed, the application of anti-inflammatory ophthalmic ointment on adult heterozygous *lncRNA-111* KO mice did not significantly improve the eye phenotype. For the accurate interpretation of this outcome, we have to consider the fact that many ocular cell types cannot regenerate[61]. Consequently, it was highly unlikely that the treatment would completely restore the eyes to the level of WT mice. This interpretation still allows the hypothesis that the KO of *lncRNA-111* alters the RPE in terms of the immune privilege. To test if earlier treatment could possibly prevent the development of eye inflammation/microphthalmia, we started the administration of enrofloxacin water to breeding pairs to minimize the risk of infections in the offspring from birth on. This experimental set-up may show us whether the phenotype is caused by bacterial inflammation.

Another explanation for the phenotype could be that *lncRNA-111* regulates a gene(s), which are essential for the development of the eye.
Microphthalmia is a disease that causes the eyes and the palpebral fissure to be significantly smaller than normal, which we observe in the heterozygous *lncRNA-111* KO mice[62]. Many genes in humans have been found to cause this disease, but as my

research showed, none of them is located closely to the candidate lncRNA (see Table 5.17). This result does not exclude the possibility that *lncRNA-111* interacts with one of them or with others that have not yet been identified.
Another possibility is that the candidate lncRNA regulates the neighboring gene *Sox9* in the retinal pigment epithelium. *Sox9* has been shown to play an important role in the activation of *BEST1* by interacting with *OXT2* and microphthalmia-associated transcription factor (*MITF*). If *BEST1* is mutated or its expression is impaired, it can cause different diseases. One of them, for example, is autosomal dominant vitreoretinochoroidopathy (ADVIRC)[45]. This disorder affects the vitreous, the retina and the choroid of the eye and can differ in severity. It can cause degeneration of the vitreous, which could be a explanation for the microphthalmia observed in heterozygous *lncRNA-111* KO mice[63].
Sox9 could also interact with the transcription factor *MITF* influencing other regulatory pathways in the eye. *MITF* consists of multiple isoforms, which have been shown to be essential for the development and survival of different cell types including the RPE. A semidominant mutation of the gene can lead to reduced pigmentation, smaller eyes and multiple other phenotypes[64]. For example, it could be possible that *Sox9* affects the splicing of the *MITF*s mRNA, causing an imbalance in the different isoforms and therefore specifically impairing the RPE.

Further research and analysis of *lncRNA-111* KO mice will allow us to define which of the above-mentioned hypotheses is correct.

6.2.1 Challenges and Outlook

Since we are at the beginning of breeding the KO mice, the main challenge analyzing the *lncRNA-111* heterozygous KO phenotype was that we could not sacrifice any of the mice. Therefore, we could not take any tissue samples for microscopic analysis of the RPE and neither could we analyze if a T cell phenotype was already present. The goal is to breed the mice to homozygous KOs and to perform microscopic analysis of the RPE and preliminary infection experiments. As soon as homozygous KO mice are available, some will be crossed with RAG2$^{-/-}$ OT-I TCR-transgenic mice and adoptive transfer experiments (as described in 6.1.5) will be performed. These experiments will allow us determine whether the microphthalmia phenotype is CD8 T cell-dependent or -independent.

7. REFERENCES

1. Murphy, K. M., Travers, P. & Walport, M. *Janeway Immunology*. *Spektrum Akademischer Verlag GmbH* **7. Aufl.,** (2009).
2. Godfrey, D. I., Kennedy, J., Suda, T. & Zlotnik, A. A developmental pathway involving four phenotypically and functionaly distinct subsets of CD3-CD4-CD8-triple-negative adult mouse thymocytes defined by CD44 and CD25 expression. *J. Immunol.* 4244–4252 (1993). doi:10.4049/jimmunol.1001782
3. Germain, R. N. T-cell development and the CD4-CD8 lineage decision. *Nat. Rev. Immunol.* **2,** 309–322 (2002).
4. Kaech, S. M. & Cui, W. Transcriptional control of effector and memory CD8+ T cell differentiation. *Nat. Rev. Immunol.* **12,** 749–761 (2012).
5. Joshi, N. S. & Kaech, S. M. Effector CD8 T Cell Development: A Balancing Act between Memory Cell Potential and Terminal Differentiation. *J. Immunol.* **180,** 1309–1315 (2008).
6. Abbas Abul K., Lichtman;, A. H. & Pillai, S. *Cellular and Molecular Immunology*. *Elsevier* **8ª ed.,** (2014).
7. Kaech, S. M. & Cui, W. Transcriptional control of effector and memory CD8+ T cell differentiation. *Nat. Rev. Immunol.* **12,** 749–761 (2012).
8. Obar, J. J. & Lefrançois, L. Memory CD8+ T cell differentiatin. **1183,** 251–266 (2010).
9. Sheridan, B. S. & Lefrançois, L. Regional and mucosal memory T cells. *Nat. Immunol.* **12,** 485–91 (2011).
10. Surh, C. D. & Sprent, J. Homeostasis of Naive and Memory T Cells. *Immunity* **29,** 848–862 (2008).
11. Cossart, P. & Toledo-Arana, A. Listeria monocytogenes, a unique model in infection biology: an overview. *Microbes Infect.* **10,** 1041–1050 (2008).
12. Hamon, M., Bierne, H. & Cossart, P. Listeria monocytogenes: a multifaceted model. *Nat. Rev. Microbiol.* **4,** 423–34 (2006).
13. Cossart, P. Illuminating the landscape of host-pathogen interactions with the bacterium Listeria monocytogenes. *Proc. Natl. Acad. Sci. U. S. A.* **108,** 19484–91 (2011).
14. Pamer, E. G. Immune responses to Listeria monocytogenes. *Nat Rev Immunol* **4,** 812–823 (2004).
15. Zenewicz, L. A. & Hao, S. Innate and adaptive immune responses to Listeria

monocytogenes: A short overview. *Microbes Infect.* **9,** 1208–1215 (2007).
16. Portnoy, D. A., Auerbuch, V. & Glomski, I. J. The cell biology of Listeria monocytogenes infection: The intersection of bacterial pathogenesis and cell-mediated immunity. *J. Cell Biol.* **158,** 409–414 (2002).
17. The ENCODE Project Consortium *et al.* An integrated encyclopedia of DNA elements in the human genome. *Nature* **489,** 57–74 (2012).
18. GENCODE Statistics http://www.gencodegenes.org/stats.html, retrieved. doi:Version 21, June 2014 freeze Ensemble 77
19. Fitzgerald, K. a & Caffrey, D. R. Long noncoding RNAs in Innate and Adaptive Immunity. 140–146 (2015). doi:10.1016/j.coi.2013.12.001.Long
20. Heward, J. a. & Lindsay, M. a. Long non-coding RNAs in the regulation of the immune response. *Trends Immunol.* 1–12 (2014). doi:10.1016/j.it.2014.07.005
21. Noncoding, L., Satpathy, A. T. & Chang, H. Y. Long Noncoding RNA in Hematopoiesis and Immunity. *Immunity* **42,** 792–804 (2015).
22. Ranzani, V. *et al.* The long intergenic noncoding RNA landscape of human lymphocytes highlights the regulation of T cell differentiation by linc-MAF-4. *Nat. Immunol.* **16,** (2015).
23. Turner, M., Galloway, A. & Vigorito, E. Noncoding RNA and its associated proteins as regulatory elements of the immune system. *Nat. Immunol.* **15,** 484–91 (2014).
24. Wang, P. *et al.* The STAT3-binding long noncoding RNA lnc-DC controls human dendritic cell differentiation. *Science* **344,** 310–3 (2014).
25. Hung, T. *et al.* Extensive and coordinated transcription of noncoding RNAs within cell-cycle promoters. *Nat. Genet.* **43,** 621–9 (2011).
26. Gomez, J. A. *et al.* The NeST long ncRNA controls microbial susceptibility and epigenetic activation of the interferon-γ locus. *Cell* **152,** 743–754 (2013).
27. Huarte, M. *et al.* A large intergenic non-coding RNA induced by p53 mediates global gene repression in the p53 response. *Cell* **142,** 409–419 (2010).
28. Carpenter, S. *et al.* A long noncoding RNA mediates both activation and repression of immune response genes. *Science (80-.).* **341,** 789–792 (2013).
29. Guttman, M. & Rinn, J. L. Modular regulatory principles of large non-coding RNAs. *Nature* **482,** 339–346 (2012).
30. Hu, G. *et al.* Expression and regulation of intergenic long noncoding RNAs during T cell development and differentiation. *Nat. Immunol.* **14,** 1190–8

(2013).
31. Wang, Y. *et al.* Long noncoding RNA derived from CD244 signaling epigenetically controls CD8 $^{+}$ T-cell immune responses in tuberculosis infection. *Proc. Natl. Acad. Sci.* **112,** E3883–E3892 (2015).
32. Stecher, C. Long non-coding RNAs and fate decisions in CD8 T cells during infection. (University of Vienna, 2015).
33. BioGPS. LncRNA 117 BioGPS. *02/10/2016* at <http://biogps.org/#goto=genereport&id=100504230>
34. Akap13 mus musculus BioGPS. *02/10/2016* at <http://biogps.org/#goto=genereport&id=75547>
35. Klhl25 BioGPS. *02/10/2016* at <http://biogps.org/#goto=genereport&id=207952>
36. Cannarile, M. a *et al.* Transcriptional regulator Id2 mediates CD8+ T cell immunity. *Nat. Immunol.* **7,** 1317–1325 (2006).
37. Yang, C. Y. *et al.* The transcriptional regulators Id2 and Id3 control the formation of distinct memory CD8+ T cell subsets. *Nat Immunol* **12,** 1221–1229 (2011).
38. BioGPS. LncRNA 111 BioGPS. *04/11/2016* at <http://biogps.org/#goto=genereport&id=72386>
39. Martin, A. B. *et al.* Gastric and colonic zinc transporter ZIP11 (Slc39a11) in mice responds to dietary zinc and exhibits nuclear localization. *J. Nutr.* **143,** 1882–1888 (2013).
40. Garside, V. C. *et al.* SOX9 modulates the expression of key transcription factors required for heart valve development. *Development* **142,** 4340–50 (2015).
41. Oh, C. Do *et al.* SOX9 regulates multiple genes in chondrocytes, including genes encoding ECM proteins, ECM modification enzymes, receptors, and transporters. *PLoS One* **9,** (2014).
42. Kadaja, M. *et al.* SOX9: A stem cell transcriptional regulator of secreted niche signaling factors. *Genes Dev.* **28,** 328–341 (2014).
43. BioGPS. Sox9. *04/11/2016* at <http://biogps.org/#goto=genereport&id=20682>
44. Poche, R. A., Furuta, Y., Chaboissier, M. C., Schedl, A. & Behringer, R. R. Sox9 is expressed in mouse multipotent retinal progenitor cells and functions in Muller glial cell development. *J. Comp. Neurol.* **510,** 237–250 (2008).

45. Masuda, T. & Esumi, N. SOX9, through interaction with microphthalmia-associated transcription factor (MITF) and OTX2, regulates BEST1 expression in the retinal pigment epithelium. *J. Biol. Chem.* **285,** 26933–26944 (2010).
46. Masuda, T. *et al.* Transcription factor sox9 plays a key role in the regulation of visual cycle gene expression in the retinal pigment epithelium. *J. Biol. Chem.* **289,** 12908–12921 (2014).
47. Sander, J. D. & Joung, J. K. CRISPR-Cas systems for editing, regulating and targeting genomes. *Nat. Biotechnol.* **32,** 347–55 (2014).
48. Ishino, Y., Shinagawa, H., Makino, K., Amemura, M. & Nakata, A. Nucleotide sequence of the iap gene, responsible for alkaline phosphatase isozyme conversion in Escherichia coli, and identification of the gene product. *J. Bacteriol.* **169,** 5429–33 (1987).
49. Jansen, R., Van Embden, J. D. A., Gaastra, W. & Schouls, L. M. Identification of genes that are associated with DNA repeats in prokaryotes. *Mol. Microbiol.* **43,** 1565–1575 (2002).
50. Makarova, K. S., Grishin, N. V, Shabalina, S. A., Wolf, Y. I. & Koonin, E. V. A putative RNA-interference-based immune system in prokaryotes: computational analysis of the predicted enzymatic machinery, functional analogies with eukaryotic RNAi, and hypothetical mechanisms of action. *Biol. Direct* **1,** 7 (2006).
51. Jinek, M. *et al.* A programmable dual-RNA-guided DNA endonuclease in adaptive bacterial immunity. *Science (80-.).* **337,** 816–821 (2012).
52. Makarova, K. S., Brouns, S. J. J., Horvath, P., Sas, D. F. & Wolf, Y. I. NIH Public Access. *Nat. Rev. …* **9,** 467–477 (2012).
53. Cong, L. & Zhang, F. in *Chromosoma Mutagenesis* (ed. Pruett-Miller, S. M.) (2015).
54. Transgenomic, I. User Guide for the Transgenomic SURVEYOR® Mutation Detection Kit for Standard Gel Electrophoresis. 1–34 (2010). at <http://www.transgenomic.com/files/literature/482106.pdf>
55. Sheridan, B. S. & Lefrançois, L. Isolation of mouse lymphocytes from small intestine tissues. *Curr. Protoc. Immunol.* 1–11 (2012). doi:10.1002/0471142735.im0319s99
56. Alberts, B. *et al. Molecular Biology of the Cell*. *4th Edition, New York* (2002).
57. Forrester, J. V. & Xu, H. Good news-bad news: The Yin and Yang of immune

privilege in the eye. *Front. Immunol.* **3,** 1–18 (2012).

58. Zhou, R. & Caspi, R. R. Ocular immune privilege. *Biol. Reports* **23410,** 2–3 (2010).
59. Zamiri, P. *et al.* Thrombospondin plays a vital mole in the immune privilege of the eye. *Investig. Ophthalmol. Vis. Sci.* **46,** 908–919 (2005).
60. Caspi, R. R. Ocular autoimmunity: The price of privilege? *Immunol. Rev.* **213,** 23–35 (2006).
61. J. Niederkorn. Mechanisms of Immune Privilege in the Eye and Hair Follicle. *JID Symp. Proc.* **8,** 168–172 (2003).
62. Cook, C. S. *Eye and Ear*. (Springer Berlin Heidelberg, 1991). doi:10.1007/978-3-642-76640-4_24
63. NCBI. autosomal dominant vitreoretinochoroidopathy - Genetics Home Reference. (2016). at <https://ghr.nlm.nih.gov/condition/autosomal-dominant-vitreoretinochoroidopathy>
64. Shibahara, S. *et al.* Microphthalmia-associated transcription factor (MITF): multiplicity in structure, function, and regulation. *J Investig Dermatol Symp Proc* **6,** 99–104 (2001).
65. Lam, M. T. Y., Li, W., Rosenfeld, M. G. & Glass, C. K. Enhancer RNAs and regulated transcriptional programs. *Trends Biochem. Sci.* **39,** 170–182 (2014).

9. ABBREVIATIONS

ActA	Actin-assembly-inducing protein
ADVIRC	Autosomal dominant vitreoretinochoroidopathy
APC	Antigen-presenting cell
ARB	Autosomal recessive bestrophinopathy
AVDM	Adult onset vitelliform macular dystrophy
Bcl2	B cell lymphoma 2, apoptosis-associated
Bcl2l11	Bcl2 like 11, apoptosis-associated
BEST1	Bestrophin 1
BFA	Brefeldin A
bp	Base pair
Cas9	CRISPR-associated protein 9
CD103	Small intestine specific tissue residency maker
CD107a	Degranulation surface marker
CD19	B cell marker
CD44	T cell activation/maturation marker
CD5	B-1 B cell marker
CD69	Tissue residency marker
cDNA	Complementary DNA
CM	Central memory
CRISPR	Clustered regularly interspaced short palindromic repeat
crRNA	CRISPR RNAs
CTLs	Cytotoxic T lymphocytes
CXCR3	T_H1 maturation marker
DN	Double negative
DNA	Deoxyribonucleic acid
dNTP	Deoxynucleotide triphosphate
DP	Double positive
DSB	Double strand breaks
DTT	Dithiothreitol
EM	Effector memory
EZH2	Enhancer of zeste homolog 2
FACS	Fluorescence activated cell sorting
FPKM	Fragments per Kilobase of transcript per Million mapped reads
GATA3	GATA binding protein 3
GZMB	Granzyme B
HDR	Homology directed repair
hnRNP-K	Heterogeneous nuclear ribonucleoprotein K
Hprt	Hypoxanthine phosphoribosyltransferase
HSC	Hematopoietic stem cells
i.v.	Intravenous
iap	Inhibitor of apoptosis gene
ICAM-1	Intercellular adhesion molecule 1
Id2	Inhibitor of DNA binding 2 gene
IFN-γ/Ifng	Interferon γ
IFNs	Type I interferons
IL-15	Interleukin 15
IL-2	Interleukin 2
IL-7	Interleukin 7
kb	Kilo base pairs
KLRG1	Killer-cell lectin like receptor G1, short lived effector T cell marker
KO	Knockout
LB	Lysogeny broth
LFA-1	Lymphocyte function-associated antigen 1
lincRNAs	Long intronic noncoding RNAs
LLO	Listeriolysin O

LM-OVA	Ovalbumin-expressing Listeria monocytogenes
lncRNA	Long noncoding RNAs
LTα	Lymphotoxin α
MHC	Major histocompatibility complex
MITF	Microphthalmia-associated transcription factor
MPECs	Memory precursor effector cells
NeST	nettoie Salmonella pas Theiler's (cleanup Salmonella not Theiler's)
NF-YA	Nuclear transcription factor Y subunit alpha
NHEJ	Non-homologous end joining
NK	Natural killer
O/N	Overnight
OVA	Ovalbumin
OXT2	Orthodenticle homeobox 2
PAMs	Protospacer adjacent motifs
PCR	Polymerase chain reaction
PMA	Phorbol 12-myristate 13-acetate
pre-TCR	Pre-T cell receptor
qPCR	Quantitative PCR
RAG2	Recombination activating gene 2
RNA	Ribonucleic acid
RNP	ribonucleoproteins
RPE	Retinal pigment epithelium
rRNA	Ribosomal RNA
RT PCR	Real time PCR
Serpinb9	apoptosis-associated
sgRNA	Single guide RNA
SI-IELs	Small intestine intraepithelial lymphocytes
SLECs	Short-lived effector precursors
snRNA	Small nucleic RNA
Sox9	Sex determining region Y box 9 gene
SSN	Single strand nicks
STAT3	Signal transducer and activator of transcription 3
TALENs	Transcriptional Activator-like Effector nuclease
T_{CM}	Central memory T cells
TCR	T cell receptor
T_{EM}	Effector memory T cells
TNF-α/Tnfa	Tumor necrosis factorα
TNFR-1	Tumor necrosis factor receptor 1
tracrRNA	Transactivating CRISPR RNAs
T_{reg}	T regulatory cells
T_{RM}	Tissue resident memory T cells
VDM	Vitelliform macular dystrophy
WDR5	WD repeat-containing protein 5
WT	Wild type
YARC	Yale School of Medicine Animal Resource Center
YFP	Yellow fluorescent protein
ZFN	Zinc finger nuclease